Petrology and magmatic evolution of the Western Sierra Chichinautzin Volcanic Field, Central Mexico

Publicado en línea el 8 de abril de 2007
Disponible en http://satori.geociencias.unam.mx/

Heterogeneous magmas of the Quaternary Sierra Chichinautzin volcanic field (central Mexico): the role of an amphibole-bearing mantle and magmatic evolution processes

Lorenzo Meriggi[1,*], José Luis Macías[1], Simone Tommasini[2], Lucia Capra[3], and Sandro Conticelli[2,4]

[1] Instituto de Geofísica, Universidad Nacional Autónoma de México, Ciudad Universitaria, Delegación Coyoacán, 04510, México D.F., Mexico.
[2] Dipartimento di Scienze della Terra, Universitá degli Studi di Firenze, Via La Pira 4, Firenze, I-5012, Italy.
[3] Centro de Geociencias, Universidad Nacional Autónoma de México, Campus Juriquilla, Apartado Postal 1-742, 76001 Querétaro, Qro., Mexico.
[4] Istituto di Geoscienze e Georisorse, Sezione di Firenze, Consiglio Nazionale delle Ricerche, Via La Pira 4, Firenze, I-50121, Italy.
** meriggi@geofisica.unam.mx*

ABSTRACT

The Quaternary Sierra Chichinautzin volcanic field (SCVF) is located at the volcanic front of the Trans-Mexican Volcanic Belt (TMVB), ~350 km from the Middle American trench where the Cocos plate subducts beneath the North American plate. The SCVF is characterized by more than 200 monogenetic centers, ranging in composition from rare basalts to dacites. Less evolved terms have aphyric to porphyritic textures with phenocrysts of euhedral olivine (± Cr-spinels inclusions) + cpx, whereas evolved terms have porphyritic textures with phenocrysts of pyroxene (cpx>opx), xenocrysts of corroded quartz, and sieve-textured plagioclase from the local basement. Regardless of the degree of magmatic evolution, plagioclase occurs as microphenocrysts or in the groundmass.

New geochemical and isotopic data presented in this work are in good agreement with previous analyses; however, a new division for the SCVF mafic rocks (MgO ≥6.0 wt.%) is proposed. In fact, although concentrations of large ion lithophile elements (LILE) and light to medium rare earth elements (REE) are roughly constant in mafic rocks, TiO_2 and other high field strength elements (HFSE) such as Nb are scattered and vary from 0.8 to 1.8 wt.% and from 5 to 30 ppm, respectively. These characteristics allow grouping the SCVF rocks in two main magmatic series with different TiO_2-HFSE enrichment: high(H)-TiO_2 and low(L)-TiO_2, with subordinate transitional samples. Additionally, a cinder cone with shoshonitic affinity and extremely high LILE/HFSE ratio is reported for the first time in central Mexico. Compositional variability is also observed among the mineral phases of these mafic rocks (e.g., the Cr# of spinel hosted in olivine phenocrysts), and the $^{87}Sr/^{86}Sr$ ratios that progressively increase from the H-TiO_2 series (0.70307–0.70425) to the L-TiO_2 series (0.70365–0.70434), up to the shoshonitic scoria (0.70456).

The calc-alkaline affinity, LILE, and Pb positive anomalies of the magmas confirm the occurrence of a subduction-related metasomatised mantle wedge beneath the studied area (particularly for the shoshonitic scoria), but enrichments in TiO_2 and other HFSE are controversial. These enrichments are not common in subduction-related magmas because these elements are not easily removed by aqueous fluids from the subducted slab. However, recent works have demonstrated that HFSE can be relatively soluble in high-temperature fluids/melts arising from the slab, and the presence of TiO_2-rich Cr-pargasite in lherzolite xenoliths of the Valle de Bravo area prove the existence of a mantle phase with high-HFSE concentrations. Therefore, partial melting of such hydrated peridotite could explain the genesis of H-TiO_2

magmas as suggested by the proposed REE model.

Moreover, isotopic ratios and variations in major and trace element concentrations of western SCVF rocks indicate that fractional crystallization plus crustal assimilation are the main evolution processes in the studied area.

Key words: volcanic rocks, high-TiO_2, Sr and Nd isotopes, magmatic evolution, Sierra Chichinautzin, Trans-Mexican Volcanic Belt, Mexico.

RESUMEN

El campo volcánico de la Sierra de Chichinautzin (CVSC) está ubicado en la porción frontal del Cinturón Volcánico Transmexicano (CVTM) a ~350 km de distancia de la Fosa Mesoamericana. El CVSC está compuesto por más de 200 centros monogenéticos cuyas rocas varían desde basaltos a dacitas. Las rocas menos evolucionadas tienen texturas desde afíricas hasta porfiríticas con fenocristales euhedrales de olivino (± inclusiones de Cr-espinela) + cpx, mientras que las rocas más evolucionadas tienen textura porfirítica con fenocristales de piroxeno (cpx>opx), xenocristales de cuarzo parcialmente reabsorbidos y plagioclasa con textura de tamiz provenientes del basamento. Independientemente del grado de evolución magmática, las plagioclasas aparecen exclusivamente en la matriz de las rocas.

Los nuevos datos geoquímicos e isotópicos de este trabajo concuerdan con estudios previos. Sin embargo, con el análisis de rocas máficas del CVSC (MgO ≥6.0% en peso) se propone una nueva subdivisión. Aunque la concentración de los elementos litófilos de radio iónico grande (LILE) y de las tierras raras (REE) ligeras y medianas es relativamente constante en las rocas máficas, el TiO_2 y otros elementos de alto potencial iónico (HFSE) como el Nb presentan una mayor variación (0.8–1.8 % en peso y 5–30 ppm, respectivamente). Estas características permiten la subdivisión de los magmas del CVSC en dos series magmáticas principales con diferentes concentraciones de TiO_2 y HFSE (series de alto(H)-TiO_2 y bajo(L)- TiO_2), además de algunas muestras de afinidad transicional. Asimismo se reporta por primera vez en el centro de México un cono de escoria con afinidad shoshonítica y relaciones elevadas de LILE/HFSE. Estas heterogeneidades composicionales se reflejan también en las variaciones del Cr# en las espinelas presentes en fenocristales de olivino y en las relaciones $^{87}Sr/^{86}Sr$ que aumentan paulatinamente de los productos de la serie H-TiO_2 (0.70307-0.70425), a aquellos de L-TiO_2 (0.70365-0.70434) hasta los valores de 0.70456 de la shoshonita.

La afinidad calcialcalina y las anomalías positivas de LILE y Pb confirman la presencia de un manto metasomatizado en el área estudiada, aunque los enriquecimientos de TiO_2 y HFSE no pueden explicarse fácilmente. Estos enriquecimientos son raros en magmas de zonas de subducción, ya que estos elementos no pueden ser transportados por fluidos a través de la cuña del manto. Sin embargo, se ha demostrado recientemente que los HFSE pueden ser relativamente solubles en los fluidos/fundidos de alta temperatura que ascienden de la placa en subducción. La ocurrencia de xenolitos peridotíticos con Cr-pargasita rica en TiO_2 en el área de Valle de Bravo confirma la existencia de una fase cristalina del manto que contiene concentraciones altas de elementos HFSE. Por lo tanto, la fusión parcial de esta peridotita hidratada podría explicar las anomalías de TiO_2 en los magmas de la CVSC, como se demuestra en el modelo presentado.

Asimismo, las relaciones isotópicas y las variaciones de los elementos mayores y trazas indican que la cristalización fraccionada acoplada a contaminación cortical son los principales procesos de evolución en el área estudiada.

Palabras clave: rocas volcánicas, high-TiO_2, isótopos de Sr y Nd, evolución magmática, Sierra de Chichinautzin, Cinturón Volcánico Trasmexicano, México.

INTRODUCTION

Magmas generated at convergent plate margins are characterized by typical chemical fingerprints: higher large ion lithophile element contents (LILE; *e.g.*, Cs, Rb, K, Ba, and Pb) with respect to high field strength element contents (HFSE; *e.g.*, Nb, Ta, Zr, and Hf) and lower FeO_{tot} relative to other sub-alkaline rocks such as MORB (*e.g.*, Gill, 1981; Wilson, 1989; Arculus, 2003). The processes that bring to these chemical characteristics are still a matter of debate, but they might be related to (1) partial melting of mantle peridotite containing a Ti-rich phase as titanate or amphibole in the residuum of partial melting (*e.g.*, Nicholls and Ringwood 1973; Hofmann 1988); or more probably to (2) partial melting processes of a mantle wedge metasomatised by fluids/melts released by the subducting slab (*e.g.*, Turner *et al.*, 1997; Walker *et al.*, 2001). Both aqueous fluids and melts from subducted sediments are capable to decrease

the solidus of the peridotite of the mantle wedge triggering partial melting (*e.g.*, Saunders *et al.*, 1980, Pearce and Peate, 1995), enriching the mantle wedge source and producing magmas with high LILE with respect to HFSE (*e.g.*, Tatsumi *et al.*, 1983; Elliott *et al.*, 1997; Patino *et al.,* 2000, Walker *et al.*, 2001). Besides, partial melting of altered subducted oceanic MORB lithosphere has been claimed for the generation of silica-rich magmas (*e.g.*, dacites and rhyolites) that produce magmatic rocks with high Sr/Y ratios and other incompatible elements, called adakites (*e.g.*, Drummond and Defant 1990; Defant and Drummond, 1990; Gómez-Tuena *et al.*, 2007). At continental plate margins, however, rhyolites with high LILE/HFSE values might also be generated by partial melting of the lower crust or by magmatic evolution of a high-alumina basaltic magma through fractional crystallization plus crustal assimilation (AFC) processes (*e.g.*, Francalanci *et al.*, 1993; Castillo *et al.*, 1999; Xu *et al.*, 2002).

The study of mantle-inherited features is a difficult task in subduction-related magmas because of the paucity of magmas that have been little modified after their genesis (primitive magmas). A magma in equilibrium with its mantle source should have Mg# values higher than 65 (Green, 1971), FeO_{tot}/MgO less than 1 (Tatsumi *et al.*, 1983), MgO ≥6 wt.% (Luhr, 1997), and Ni = 235–400 ppm (Sato, 1977), characteristics rather unusual in many arc-related magmas.

At convergent plate margins, besides typical arc magmas (*e.g.*, arc tholeiites, calc-alkaline), alkaline mafic magmas with either subduction-related or intra-plate characteristics can be found (*e.g.*, van Bergen *et al.*, 1992; Green, 2005). Potassic and ultrapotassic magmatic rocks with evident HFSE depletion have been found in central Italy (*e.g.*, Conticelli and Peccerillo, 1992; Conticelli 1998; Conticelli *et al.*, 1997, 2002, 2007), in the Aeolian Arc, south Italy (*e.g.*, Francalanci *et al.*, 1993, 1999, 2004), in the Sunda-Banda Arc (*e.g.*, van Bergen *et al.*, 1992) and in the Trans-Mexican Volcanic Belt (*e.g.*, Carmichael *et al.*, 1996). On the other hand, OIB-like alkali basalts have been found in the Cascade Range (*e.g.*, Reiners *et al.*, 2000; Smith and Leeman, 2005); high-TiO_2 lavas are present in the Central America volcanic arc (*e.g.*, Walker *et al.*, 1990); and intra-plate alkaline magmas have been found in the Trans-Mexican Volcanic Belt (*e.g.*, Luhr, 1997; Ferrari *et al.*, 2000). Production of magmas with transitional to OIB-like geochemical characters at convergent plate margins have been explained as follow: 1) different magma genesis mechanisms, *e.g.*, flux *vs.* decompressional melting (*e.g.*, Reiners *et al.*, 2000); 2) mantle heterogeneity at small scale (*e.g.*, Feigenson and Carr, 1993; Strong and Wolff, 2003); 3) roll-back of the subducted plate with slab window opening (Ferrari *et al.*, 2001); 4) continental rifting (*e.g.*, Verma, 2000, 2002); 5) uprise of a deep-seated mantle plume (*e.g.*, Márquez *et al.*, 1999a, 199b; Márquez and De Ignacio, 2002).

In this context, the Sierra Chichinautzin volcanic field (SCVF) (Figure 1) represents a unique site to perform petrological and geochemical studies to address the problem of contemporaneous presence of within-plate and subduction-related magmas at a destructive plate margin because of the abundant presence of fairly primitive magmas (MgO ≥6.0 wt.%), with different LILE/HFSE ratios, despite the thickness of the continental crust (~45 km, *e.g.*, Urrutia-Fucugauchi and Flores-Ruíz, 1996). The aim of this paper is to investigate the magma genesis and the evolution processes of the Tenango area, located in the westernmost SCVF, between the late Pliocene Sierra de Las Cruces volcanic chain (Figure 1c; Bloomfield, 1974, 1975; Osete *et al.*, 2000) and the late Pliocene to Holocene Nevado de Toluca volcano (García-Palomo *et al.*, 2002a), where both primitive magmas and evolved lava flows coexist. Although this area has been previously studied by other authors (Bloomfield, 1974; 1975; García-Palomo *et al.*, 2000; 2002a; Martínez-Serrano *et al.*, 2004) we present new geochemical and petrographic data of Chapultepec, Villa Metepec, Emerenciano and Sta. Cruz cinder cones and a more exhaustive sampling of Texontepec and the Tenango lava flow (Figure 1c).

GEOLOGICAL BACKGROUND

The Trans-Mexican Volcanic Belt (TMVB) is a 1,200-km long volcanic chain that transects Mexico from the Pacific Ocean to the Gulf of Mexico (Figure 1a). The oldest Trans-Mexican Volcanic Belt products are Miocene in age and form a widespread mafic to intermediate volcanic arc with calc-alkaline to slightly alkaline affinity (Ferrari *et al.*, 2000). Miocene to present-day volcanism in the TMVB consists of large stratovolcanoes and dispersed monogenetic volcanic centers that have erupted calc-alkaline, Na-alkaline and K-alkaline magmas. In some regions the monogenetic cones are associated with polygenetic volcanoes (*e.g.*, Colima volcano; Luhr and Carmichael, 1981), but in other regions they are scattered to form extended volcanic fields as in Michoacán-Guanajuato (Hasenaka and Carmichael, 1985; Luhr and Carmichael, 1985), Zitácuaro-Valle de Bravo (Blatter and Carmichael, 1998a, 1998b, 2001), Los Tuxtlas (Nelson and González-Caver, 1992), Apan-Tezontepec (García-Palomo *et al.*, 2002b), and Sierra Chichinautzin (Bloomfield, 1974, 1975; Swinamer, 1989; Martín-del Pozzo, 1982; Wallace and Carmichael, 1999; Verma, 1999, 2000; Velasco-Tapia and Verma, 2001a, 2001b; Márquez and De Ignacio, 2002; Cervantes and Wallace, 2003a, 2003b; Martínez-Serrano *et al.*, 2004; Siebe *et al.*, 2004a, 2004b, 2005).

The SCVF is a volcanic area of about 2,400 km^2 bounded by the Sierra Nevada to the east and by the Nevado de Toluca volcano to the west. Nevado de Toluca volcano has an efficient volcanic plumbing system controlled by the intersection of three important tectonic features: the San Antonio fault system, the Taxco–Querétaro fault system,

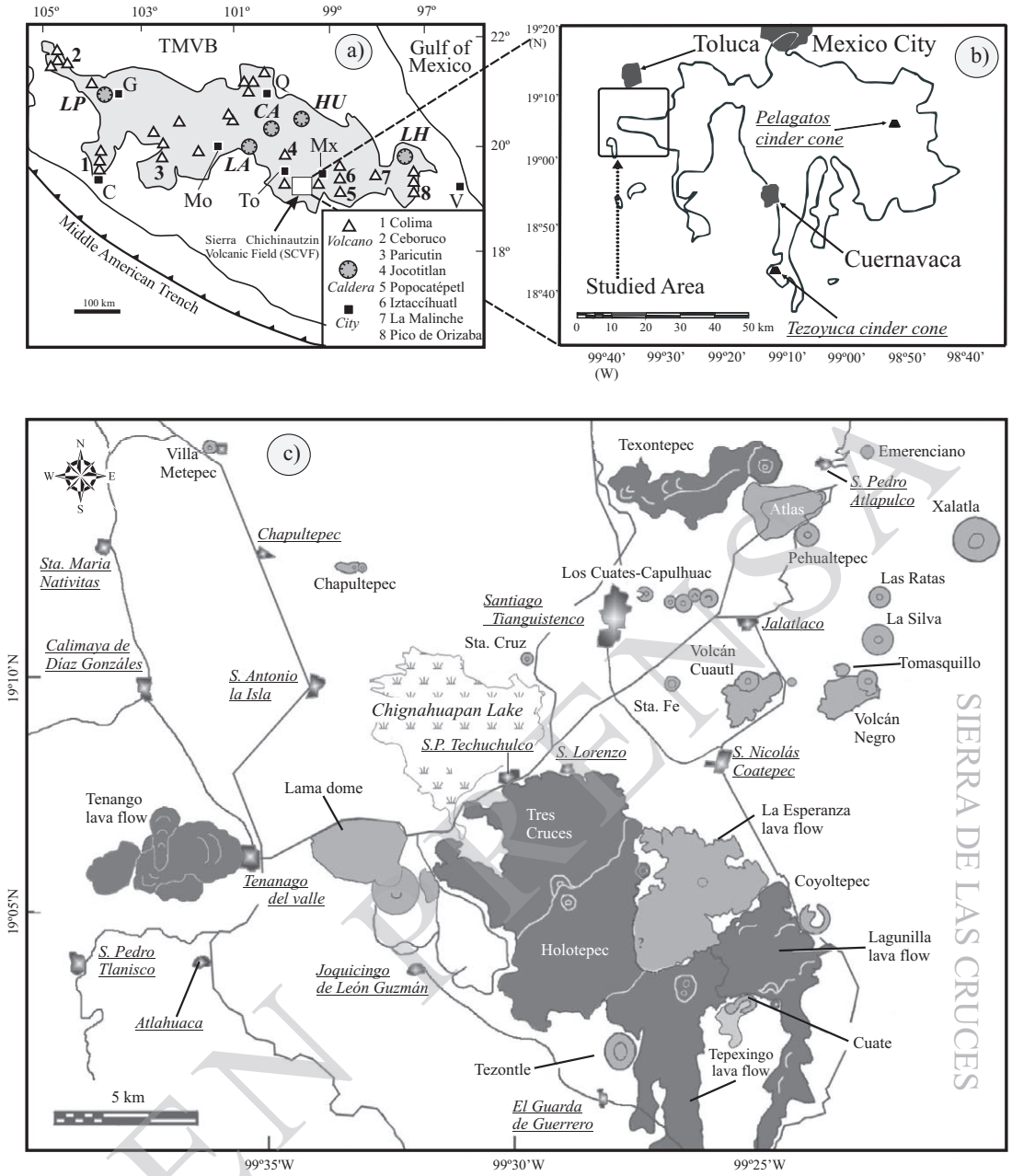

Figure 1. a: Sketch map of the Trans-Mexican Volcanic Belt. Calderas: *LP*: La Primavera; *LA*: Los Azufres; *CA*: Amealco; *HU*: Huichapan; *LH*: Los Humeros. Cities: G: Guadalajara; Mo: Morelia; Q: Querétaro; To: Toluca; Mx: Mexico City; V: Veracruz. Modified from Arce *et al.* (2003). b: Location of the Sierra Chichinautzin volcanic field (SCVF) shown in a). Modified from Bloomfield (1974). c: Simplified geological map of the Tenango area. Darker areas are post-UTP products, lighter areas are pre-UTP products. Modified from García-Palomo *et al.* (2002a).

and the Tenango fault system, which that also feeds the monogenetic lava flows of the western portion of the SCVF (García-Palomo *et al.*, 2000). The SCVF is characterized by more than 200 scattered monogenetic centers, mainly scoria cones with associated lava flows, shield volcanoes, and minor fissural lava flows and domes (Martín-del Pozzo, 1982; Márquez *et al.*, 1999a, 1999b).

The chronology of the SCVF magmatic rocks is poorly known. Only about 8 % of the SCVF products have been dated by ^{14}C, therefore the age of the beginning of volcanic activity is still unknown (Bloomfield, 1975; García-Palomo *et al.*, 2000a; Siebe *et al.*, 2004a and references therein). This problem limits the accuracy of estimations of the effusion rates at the volcanic front of this part of the Trans-Mexican Volcanic Belt and makes difficult to understand the relationship between monogenetic activity and the older volcanic products.

In the western portion of the SCVF, in the vicinity of

the Tenango village, the products of monogenetic activity are interbedded with pyroclastic deposits of the Nevado de Toluca volcano, such as the 10.5 ka Upper Toluca Pumice (UTP; Figure 1c; Arce *et al.*, 2003; García-Palomo *et al.*, 2002a). A few geochronological data of these products provide ages between 38.6 and 19.5 ka for the ancient cones (pre-UTP phase: Tezontle, Pehualtepec, Chapultepec, Villa Metepec, Volcán Emerenciano, La Silva, Tomasquillo, Volcán Negro, Volcán Cuautl, Volcán La Mesa, Los Cuates-Capulhuac system, Lama dome and La Esperanza lava flow) and around 8.5 ka for Tenango, Tres Cruces-Holotepec, Tepexingo, Texontepec and Lagunilla lava flows (post-UTP phase; Bloomfield, 1974, 1975; Meriggi, 1999; García-Palomo *et al.*, 2000).

Previous works (*e.g.*, Wallace and Carmichael, 1999 and Verma, 2000) showed that the mafic SCVF rocks are characterized by chemical heterogeneity and include products with both calc-alkaline and OIB-type affinity, whose origin is still under debate. For the aim of this work, we use the Tezoyuca cinder cone as the primitive end-member of the OIB-type magmatic series, and the Pelagatos cinder cone as representative of the low(L)-TiO_2 series, in agreement with Márquez and De Ignacio (2002) (Figure 1b).

ANALYTICAL TECHNIQUES

Forty one samples were analyzed for major and trace elements at the Dipartimento di Scienze della Terra of the Università degli Studi di Firenze (Italy) by X-Ray Fluorescence (XRF) with a Philips PW 1480 spectrometer using the Franzini *et al.* (1972) method, along with several trace elements. International reference samples and internal standards were used to evaluate accuracy and precision. The uncertainty for trace elements was estimated to be less than 10% for Y, Nd, Ba, Nb, and Cr, and less than 5% for all other trace elements. MgO, K_2O and Na_2O contents were determined by Atomic Absorption Spectrometry (AAS). FeO was determined by titration following Shapiro and Brannock (1962), and lost on ignition (LOI) by the gravimetric method.

Nineteen samples (d-10, d-25, d-37, d-42, d-45, d-47, d-50, d-51, d-53, d-54, d-56, TEB, Sc02, Sc05, Sc08, Sc09, Mx14, XTN and L2) were analyzed for major, trace and REE elements by Inductively Coupled Plasma Emission Spectrometry (ICP-ES) and Instrumental Neutron Activation Analysis (INAA) at Activation Laboratories, Ancaster, Canada. The analytical error was less than 0.01% for major and trace elements (Ba, Cr, Cu, Ni, Sr, Ta, V, Y, Zn); less than 1 ppm for Zr; 0.5 ppm for Cs, Hf, Tb, U; and 20 ppm for Rb. The detection limit for Sm, Eu, and Yb was 0.1 ppm.

Mineral chemistry was detrmined at the C.N.R., Istituto di Geoscienze e Georisorse of Firenze (Italy) by using a JEOL JXA 8600 automated microprobe using 15-kV accelerating voltage and 10-nA beam current with variable counting times. Matrix correction was performed using the Bence and Albee (1968) and Albee and Ray (1970) method. Analytical errors are similar to those reported by Vaggelli *et al.* (1999).

Sr and Nd isotope analyses were performed at the Dipartimento di Scienze della Terra of Firenze (Italy) using a Thermo Finnigan Triton-Ti thermal ionization mass spectrometer equipped with nine movable collectors (Avanzinelli *et al.*, 2005). Sample powder (100–150 mg) was dissolved in a HF-HNO_3-HCl mixture. Sr and Nd fractions were separated at the LUGIS laboratory of Instituto de Geofísica and Instituto de Geología, UNAM, Mexico City (Mexico) following standard chromatographic techniques using AG50W-X12 and PTFE-HDEHP resins with HCl as solvent. The total procedural blank was <5 ng for Sr and <2 ng for Nd, making blank correction negligible. Sr and Nd isotope compositions were measured in dynamic mode and are reported normalized to $^{86}Sr/^{88}Sr = 0.1194$ and $^{146}Nd/^{144}Nd = 0.7219$, respectively. Exponential-law mass fractionation correction was used for all Sr and Nd isotopic data. Uncertainties in measured (m) isotopic ratios refer to the least significant digits and represent $\pm 2\sigma$ in-run precision. The external precision of NIST SRM987 was $^{87}Sr/^{86}Sr = 0.710251 \pm 10$ (2σ, n = 39), and that of the La Jolla standard was $^{143}Nd/^{144}Nd = 0.511845 \pm 4$ (2σ, n = 11).

PETROGRAPHY OF LAVAS AND XENOLITHS

Modal abundance of 12 representative samples was determined with the point counting method. Phenocrysts (Ph) are defined as crystals >0.3 mm, microphenocrysts (MPh), those between 0.3 and 0.03 mm, and groundmass (glass and microliths) those phases less than 0.03 mm. In the following sections we describe these rocks in groups defined by MgO contents and crustal xenoliths. Generally mafic samples are porphyritic with abundant pheno- and microphenocrystals of olivine and less abundant pyroxene (clinopyroxene>orthopyroxene). In more evolved rocks olivine is progressively substituted by orthopyroxene and xenocrysts/xenoliths of foreign provenance are fairly common. These mineral associations are similar to those described by Márquez and De Ignacio (2002); representative modal analyses of mafic to evolved samples are reported in Table A1in the electronic supplement.

Mafic magmas (MgO ≥6.0)

Mafic rocks (*e.g.*, Los Cuates-Capulhuac system) have a porphyritic index (P.I.) between 10–15 vol. % with abundant phenocrysts of euhedral olivine, dotted by Mg-chromite inclusions (rarely partially altered to iddingsite) ± clinopyroxene (Table A1). The same mineral phases appear in the groundmass along with microphenocrysts of plagioclase, opaque minerals and abundant clear to brown glass.

Glomeroporphyritic aggregates of olivine + clinopyroxene are relatively abundant. These rocks contain rare quartz-bearing xenoliths or, when disaggregated, isolate quartz xenocrysts surrounded by clinopyroxene coronas, whereas orthopyroxene coronas are found around olivine phenocrysts. Scoria from the Sta. Cruz cinder cone (samples Mx11 and d-10) represents an exception among mafic magmas due to the absence of olivine as a phenocryst phase. Euhedral clinopyroxene is the only phenocryst observed, and is embedded in a groundmass composed of microcrystals of pyroxene, apatite, glass and rare clinopyroxene glomeroporphyritic assemblages. As in other pre-UTP samples, plagioclase is observed only as microliths in the groundmass.

Intermediate to felsic magmas (MgO <6.0 wt %)

Intermediate rocks constitute an isolated cinder cone (*e.g.*, Chapultepec) and thick lava flows (Tenango, Tepexingo, Lagunilla) or small shield volcanoes (Tres Cruces/Holotepec) (Figure 1c). These rocks are characterized by the highest porphyritic index (P.I.) ≤15 vol. %, with sparse phenocrysts and microphenocrysts of olivine, generally without spinel inclusions, orthopyroxene and clinopyroxene microphenocrysts. The groundmass consists of glass and abundant microliths of plagioclase and opaque minerals arranged in trachytic textures. These lavas are also characterized by abundant xenocrysts of deeply resorbed, centimeter-sized plagioclase with sieve texture and thin overgrowths, ghosts of relict hornblende, clinopyroxene-rimmed quartz and almost totally resorbed subcentimetric clinopyroxene.

Felsic rocks (*e.g.*, La Esperanza lava flow) have aphyric textures (P.I. <5 vol. %) with sparse microphenocrysts of orthopyroxene set in a felsic microcrystalline groundmass made of thin laths of plagioclase.

Crustal xenoliths

The Lama dome and Tenango lavas host two types of xenoliths of heterogeneous size and provenance. The first type consists of centimetric-sized green conglomerates common in the southernmost part of the Tenango andesite (sample XTN). In thin section they show a clastic texture made of sub-angular grains (<0.3 mm) constituted by feldspar, pyroxene, calcite, and dolomite set in a groundmass of chlorite, calcite and sparce epidote.

The second type consists of light-gray centimetric-sized quartz-diorites, common in the Lama dome. These xenoliths have ovoidal shapes surrounded by thin (~0.5 mm) dark rims in contact with the host lava. They show coarse equigranular texture with disequilibrium features, especially close to the contact with the host magmas. They are constituted by clinopyroxene, anhedral quartz (≤1 cm in length) with undulate extinction and annealing texture, zoned and twinned plagioclase with accessory zircon, mafic phases (biotite?) completely substituted by fine aggregates of spinel and hercynite, and abundant rhyolitic glass with variable amounts of K_2O. Minor ilmenite, sillimanite and rare titanite are present too, as revealed by electron microprobe analysis. The petrographic and chemical characteristics of these xenoliths are similar to the dioritic intrusive body of the Guerrero Terrane described by De Cserna *et al.* (1974).

MINERAL CHEMISTRY

Olivine. Crystals observed in rocks from the western SCVF are Fo_{87-81} with euhedral and rarer skeletal habits. They are slightly normally zoned (3–10 Fo mol. %; Table A2 in the electronic supplement). More fayalitic olivine (Fo_{79-65}) occurs in the groundmass as microphenocrysts. No evident differences exist in the major element composition of the analyzed olivine crystals, but the Tenango lava phenocrysts are always rimmed by thin laths (<5 μm) of orthopyroxene.

Equilibrium between melt and olivine was tested by plotting the whole-rock Mg# *vs.* Fo content of olivine (Figure 2). The exchange distribution coefficient ($K_D = [X_{FeO}/X_{MgO}]^{Olivine}/[X_{FeO}/X_{MgO}]^{Liquid}$) following Toplis (2005) yield values of 0.36–0.38, in agreement with previous works (*e.g.*, Wallace and Carmichael, 1999). As shown in Figure 2, olivine phenocryst cores straddle the equilibrium

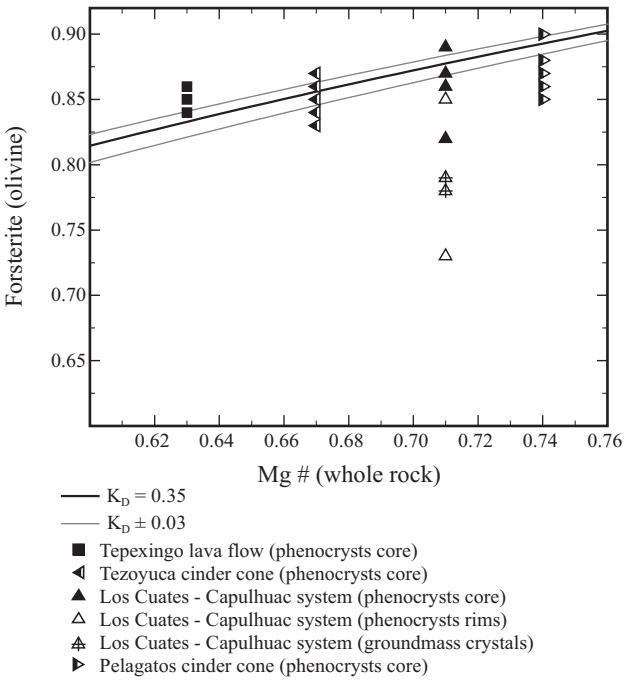

Figure 2. Forsterite content of olivines *vs.* whole-rock Mg# (calculated after Frey *et al.*, 1978). The curves represent equilibrium Fe-Mg partitioning between olivine and melt corresponding to K_D of 0.35±0.03 in agreement with Toplis (2005).

line whereas phenocryst rims and groundmass crystals are Fo-poor and fall slightly above the line, suggesting late crystallization.

Clinopyroxene. This is the second most abundant phase in the mafic rocks (Table A3 in the electronic supplement.). Clinopyroxene phenocrysts show fairly constant compositions with $En_{42-52}Wo_{35-42}$ (Figure 3) and are usually normally zoned up to 10 mol. % in En. In intermediate to evolved lavas as the Tenango andesite, clinopyroxene microcrysts are also present as rims around quartz xenocrysts and show similar En contents but lower Al_2O_3 (Table A3).

Rare unstable clinopyroxene phenocrysts occur in the crustal xenoliths collected at the Lama dome, which have constant compositions of $En_{42-36}Wo_{38-41}$, variable Al_2O_3 contents (0.7–2.2 wt.%), and low Cr_2O_3.

Phenocrysts of clinopyroxene also occur in the Sta. Cruz cinder cone with cores of constant composition ($En_{49-40}Wo_{42-46}$) and strong normal zoned rims up to 20% in enstatite.

Orthopyroxene. This mineral phase is not common in magmas of the western SCVF, and only a few phenocrysts are observed. It commonly appears as microphenocrysts or as rims in olivine phenocrysts, in particular in intermediate to evolved samples with remarkably constant compositions (En_{84-62}) and normal zoning of up to 24 % in enstatite (Figure 3 and Table A3). In the crustal xenoliths of the Lama dome and Tenango lavas, orthopyroxene is less enriched in MgO (En_{66-55}) and have higher values of Al_2O_3 (up to 7.83 wt.%) and FeO, but with very low Cr_2O_3.

Hornblende. The Tenango lava flows and the Lama dome show a widespread presence of ghosts of euhedral hornblende (up to 0.5 mm) totally replaced by minute oxide

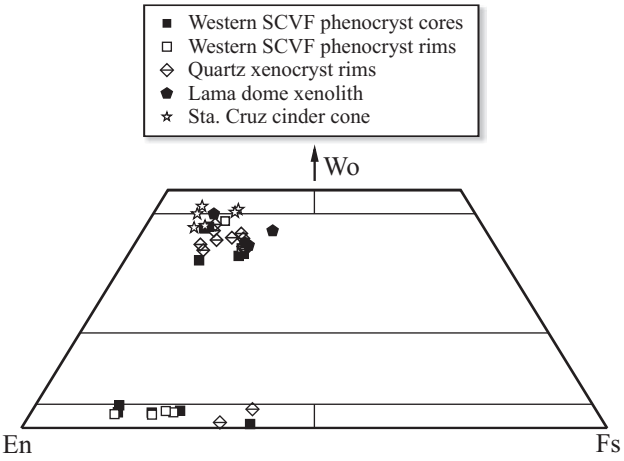

Figure 3. Pyroxene classification after Morimoto (1989) for crystals analysed in some rocks and xenoliths of the western SCVF. Most clinopyroxenes have similar compositions, whereas orthopyroxene of quartz xenocryst rims show slight enrichments in ferrosilite with respect to other samples. Wo: wollastonite, Fs: ferrosilite, En: enstatite.

aggregates unsuitable for microprobe analysis. Therefore, it is difficult to interpret their origin (*e.g.*, phenocrysts *vs.* xenocrysts), although tschermakitic as well as Mg-hastingsitic hornblende have been reported in the central and eastern portion of the SCVF by Velasco-Tapia (2002).

Plagioclase. One of the main features of SCVF rocks is the absence of plagioclase phenocrysts although it represents the main mineral phase in the groundmass. Most plagioclase has labradoritic core compositions (Table A4 in the electronic supplement. and Figure 4). Few grains are large enough for multiple analyses with the electron

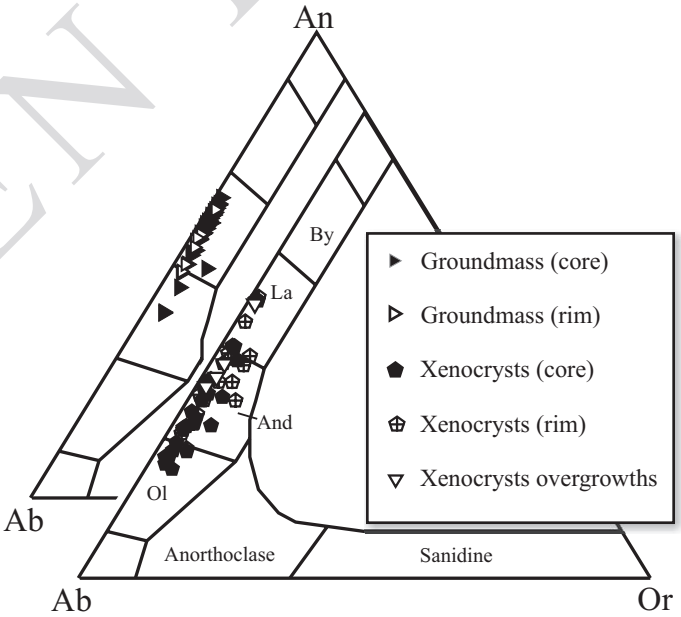

Figure 4. Compositional variation of groundmass plagioclase of western SCVF magmas (behind) and xenocrystic plagioclase of the Tenango andesite and Lama dome. An: anorthite, By: bytownite, La: labradorite, And: andesine, Ol: oligoclase, Ab: albite, Or: orthoclase.

microprobe and show a slight normal zoning with compositions between An_{64} and An_{50}. Millimeter to centimeter-long plagioclase crystals (up to 1.5 cm in diameter) observed in the Tenango lava and Lama dome show thick sieve-textured rims, cores with lower CaO contents (An_{42-29}), and thin (~2 μm) unresorbed overgrowths with anorthite contents similar to those of the groundmass laths (Table A4 and Figure 4).

Oxides. Opaque phases are common in the primitive products of the pre-UTP rocks (*e.g.*, Los Cuates-Capulhuac system; Figure 1c) and also are observed in few intermediate rocks (*e.g.*, Tepexingo). They are Mg-chromites and less abundant spinels, with variable Cr# (0.45–0.68), whereas spinels, Ti-magnetite, and ilmenites are common in the groundmass of all analyzed lavas. The xenoliths from the Lama dome contain abundant sub-idiomorphic spinels and hercynite that are interpreted as the result of reaction of ancient mafic phases (Table A5 in the electronic supplement.).

WHOLE ROCK CHEMISTRY

We have analyzed 60 samples of lava flows, scoriae, domes, and two crustal xenoliths (Table A6 in the electronic supplement.). Several authors (*e.g.*, Wallace and Carmichael, 1999; Siebe *et al.* 2004b; Schaaf *et al.*, 2005) described the presence of alkaline magmas in the SCVF by using the MacDonald and Katsura (1964) line. However, by using the Irvine and Baragar (1971) line it is clear that most samples have a sub-alkaline affinity (Figure 5) and only a few samples have a mild alkaline affinity (also enriched in HFSE and other incompatible elements). Tezoyuca (d-37) and Pelagatos (d-25) cinder cone rocks were included in this study for references purposes (Table A6), because they were considered as representative of the calc-alkaline and OIB-like magmatic series of the SCVF (Márquez and De Ignacio, 2002).

Intermediate to evolved samples of the SCVF have similar chemical characteristics, however, mafic samples with MgO ≥6.0 wt.% are more heterogeneous. By using their HFSE contents it is possible to discriminate between a high(H)-TiO_2, and a low(L)-TiO_2 magma series, as well as a few transitional products (Figure 6). In this Figure, most of the mafic samples from western Sierra Chichinautzin display a H-TiO_2 to transitional affinity, although they do not extend to the highest H-TiO_2 contents found elsewhere in the SCVF. In the total alkali *versus* silica diagram of Figure 5 the analyzed samples are in good agreement with previous works following a linear trend from basalts (Los Cuates-Capulhuac system, 52.3 – 53.5 wt.% SiO_2) to dacites (La Esperanza, 60.3 – 66.0 wt.% SiO_2). The western SCVF magmas follow the typical calc-alkaline trend on the AFM diagram (although this kind of diagram should be used with caution, Sheth *et al.*, 2002) and plot in the medium-K field of the K_2O *versus* silica diagram of Peccerillo and Taylor (1976) of Figure 7. All but two samples are *hy*-normative

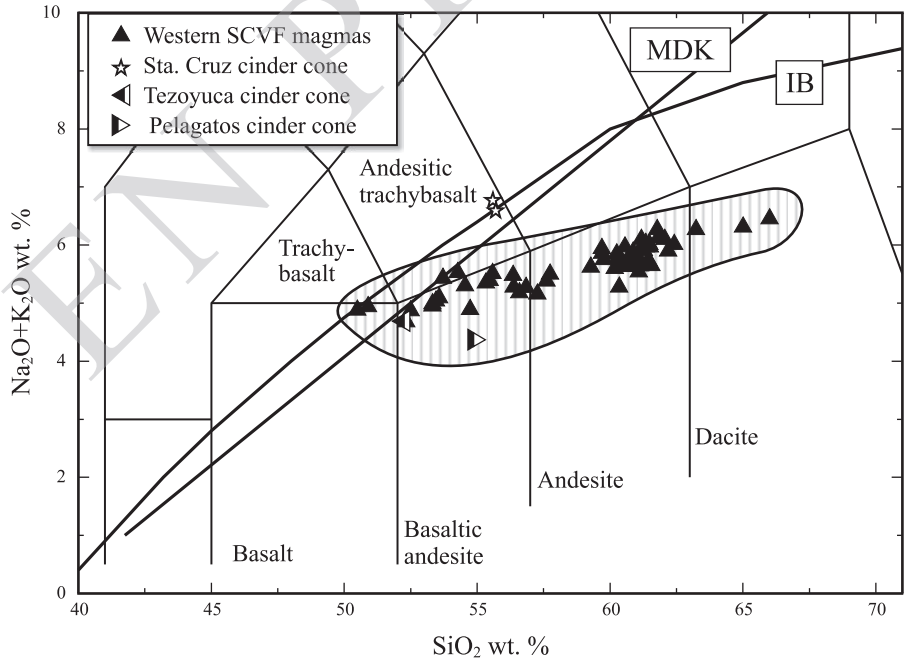

Figure 5. Total Alkali *vs.* Silica (TAS) classification diagram (Le Bas *et al.*, 1986). Lines that separate alkaline from sub-alkaline products after MDK: MacDonald and Katsura (1964), and IB: Irvine and Baragar (1971). No clear alkaline products are found, although a few mafic rocks and the Sta. Cruz cinder cone straddle the IB line. Analyses are recalculated to 100% on water free basis with total iron as FeO. The filled area represents the entire SCVF compositional range (data from Nixon, 1988; Swinamer, 1989; Wallace and Carmichael, 1999; Verma, 1999, 2000; Velasco-Tapia and Verma, 2001a, 2001b; Velasco-Tapia, 2002; Siebe *et al.*, 2004b; and Schaaf *et al.*, 2005).

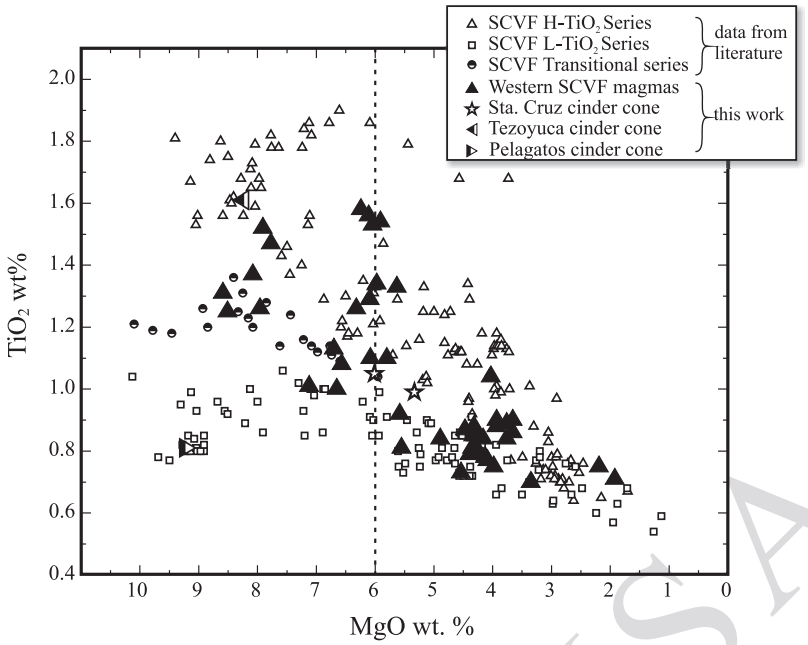

Figure 6. Discrimination diagram for the SCVF magmas showing different magmatic series with variable contents in TiO_2. Data provenance as in Figure 5.

according to the CIPW calculation (Table A6). Moreover, as noticed by Wallace and Carmichael (1999), an important feature of the studied rocks is their high concentration of MgO at given silica contents. For instance, andesites of the SCVF have MgO contents of 5.39 – 9.38 wt.%, higher than typical values of calc-alkaline andesites (*e.g.*, <4.4 wt.%, Gill, 1981; Wilson, 1989). These high-MgO andesites are relatively uncommon but they have been found at subduction-related environments (*e.g.*, Shimoda *et al.*, 1998; Tatsumi, 2001).

The Santa Cruz cinder cone is anomalous in composition as compared to other samples from the SCVF. It has higher K_2O contents that plot in the shoshonitic field of Figure 7. Although Wallace and Carmichael (1999) previously reported high-potassium magmas in the western SCVF (*e.g.*, Cerro el Perico near the city of Toluca, Figure 7), the Santa Cruz cone is the first shoshonitic cone found in central Mexico.

Incompatible element pattern diagrams of representative mafic magmas (MgO ≥6.0 wt.%) of the transitional and L-TiO_2 series of the western SCVF and the Sta. Cruz cinder cone are shown in Figure 8a. The Sta. Cruz cinder cone shows anomalous enrichments in almost all incompatible elements. The other magmas from the Tenango area display similar patterns with clear troughs at Ta, Nb and Ti, and positive anomalies of Ba, Pb and Sr. All these characteristics are also observed in the multielement diagrams of Figure 8b, that shows the Pelagatos cinder cone and other subduction-related mafic magmas from different sectors of the Trans-Mexican Volcanic Belt (*e.g.*, Cerro Colorado, Siebert and Carrasco-Núñez, 2005; and monogenetic products from Mascota, Carmichael *et al.*, 1996), as well as in the Stromboli and Alicudi magmas from the Aeolian Arc, Italy (Francalanci *et al.*, 1993). As shown in Figure 8c, similar enrichments in Ba, Pb and Sr appear also in the multielement diagrams of the so-called OIB magmas from Garibaldi Volcanic Belt (northern Cascadia; Green, 2005) and the H-TiO_2 magmas of the SCVF (Tezoyuca and Tepetlapa cinder cones). However, it is worth mentioning that such characteristics are absent in the multielement diagrams of typical OIB magmas as those from Galapagos Islands (Reynolds and Geist, 1995) and Tubuai island (Chauvel *et al.*, 1992).

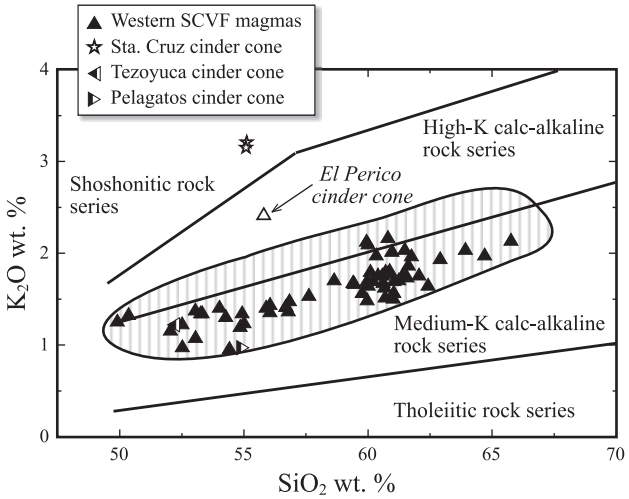

Figure 7. K_2O wt.% *vs*. SiO_2 wt.% diagram for the western SCVF rocks. Classification lines after Peccerillo and Taylor (1976). El Perico cinder cone is sample 292 of Wallace and Carmichael (1999). Data provenance and symbols as in Figure 5.

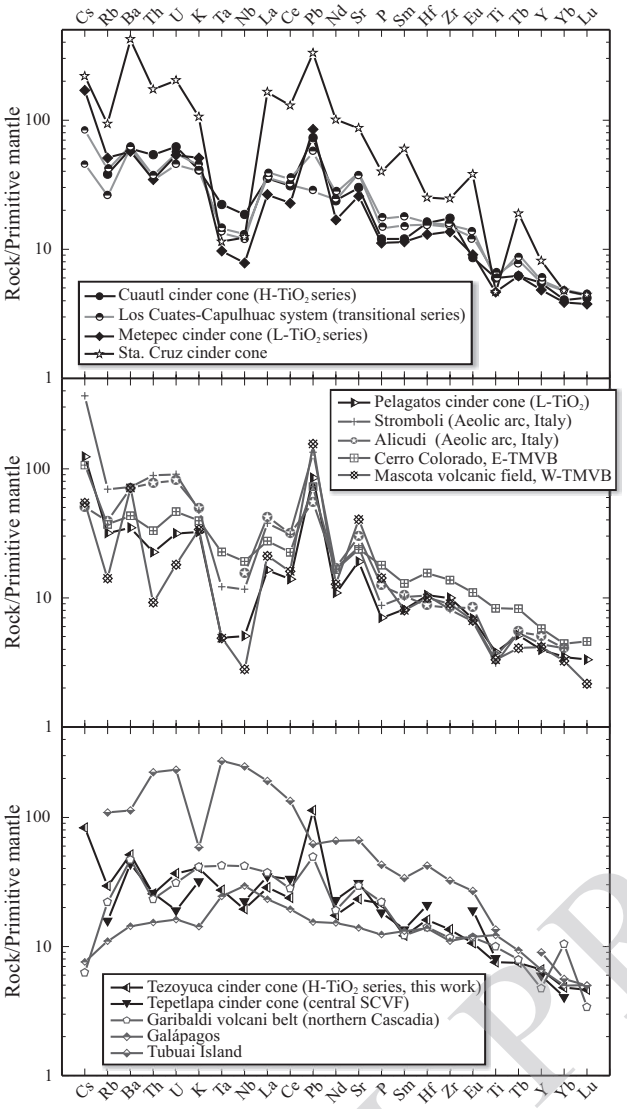

Figure 8. a: Multielement diagram of representative rocks of the Tenango area. b: Multielement diagram of the Pelagatos cinder cone (L-TiO_2 series, this work) and other subduction-related magmas from the Aeolian arc (Francalanci *et al.*, 1993); Cerro Colorado cinder cone, eastern Trans-Mexican Volcanic Belt (Siebert and Carrasco-Núñez, 2005); and the Mascota volcanic field, western TMVB (Carmichael *et al.*, 1996). c: Multielement diagram of the Tezoyuca cinder cone (H-TiO_2 series, this work), Tepetlapa cinder cone (Cervantes and Wallace, 2003a), Galapagos basalt (Reynolds and Geist, 1995) and a typical HIMU basalt (Tubuai island; Chauvel *et al.*, 1992). Notice that most Mexican magmas display slight to clear negative anomalies of Ta, Nb and Ti, and positive anomalies of Pb and Sr, as compared to the OIB lavas. Only mafic rocks (MgO ≥6.0 wt.%; on recalculated water free basis) are considered. Normalization values for primitive mantle are from Sun and McDonough (1989), whereas incompatible elements order is taken from Hofmann (1988).

The REE distribution in mafic samples of the Tenango area show similar patterns with slight enrichments in light REE [$(La/Lu)_N$ = 7.0–10.0] and nearly flat heavy REE alignments. The Sta. Cruz cone shows higher values for the light to medium REE, whereas Tm, Yb and Lu abundances are comparable to those of the other samples (Figure 9).

Sr and Nd isotopes

Isotopic data for the H-MgO SCVF samples are sparse and only a few rocks have been studied in some detail. New (Table 1) and previously reported data show that mafic magmas (MgO ≥6.0 wt%) belonging to the H- and L-TiO_2 series show very similar $^{143}Nd/^{144}Nd$ ratios (0.51274–0.51298), but greater differences can be found in the $^{87}Sr/^{86}Sr$ ratio (Figure 10), although some overlap between samples from different series exist. Particularly, most mafic L-TiO_2 rocks gather in the right side of the mantle array due to their enrichment in radiogenic Sr ($^{87}Sr/^{86}Sr$ >0.7041), with respect to the H-TiO_2 mafic rocks (Figure 10). The high K_2O rocks of Sta. Cruz cinder cone (sample d-10, MgO = 5.33 wt.%) show even a stronger enrichment in radiogenic Sr, with $^{87}Sr/^{86}Sr$ ratios falling outside of the mantle array of Figure 10. The xenoliths L2 and XTN (Table A6) fall inside the mantle array as well as the high-SiO_2 andesites and dacites from nearby stratovolcanoes of Nevado de Toluca and Popocatépetl (Figure 10b).

DISCUSSION

Magma genesis

The bulk rock composition of the mafic SCVF magmas is characterized by important variations in TiO_2 and HFSE represented by rocks belonging to three magmatic series: L-TiO_2, intermediate-TiO_2, and H-TiO_2 (Figure 6). These chemical variations are also observed in the composition of spinels hosted in olivine phenocrysts at given Fo contents (Figure 11). If the Cr# is used, it is clear that the spinels of Pelagatos cinder cone (L-TiO_2 series) have higher values than the spinels from Tezoyuca cinder cone

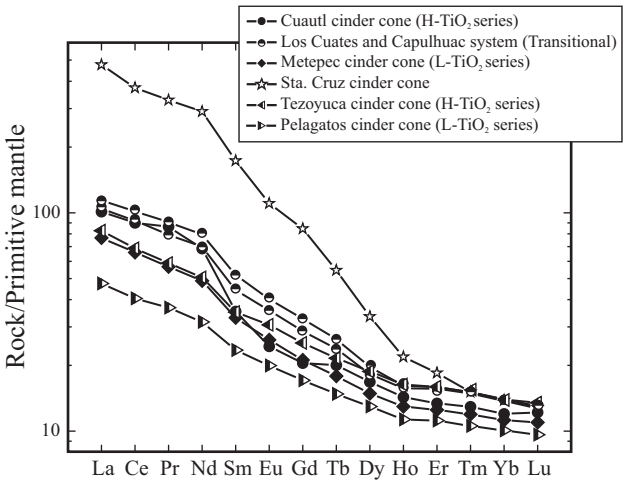

Figure 9. Rare Earth Elements for mafic rocks (MgO ≥6.0 wt.% on recalculated water free basis) of the Tenango area plus Tezoyuca and Pelagatos cinder cones. Normalization follows primitive mantle values of Sun and McDonough (1989).

Table 1. Sr and Nd isotopic compositions of analyzed samples from the western Sierra Chichinautzin volcanic field.

Locality	Sample	MgO (wt.%)	Latitude N	Longitude W	Affinity	$^{87}Sr/^{86}Sr$	$\pm2\sigma_m$	$^{143}Nd/^{144}Nd$	$\pm2\sigma_m$	εNd
Sta. Cruz	**d-10**	5.33	19°10'18.0"	99°29'44.0"	H-K_2O	0.70456	8	0.51295	7	6.0
Metepec	**d-50**	7.12	19°14'57.1"	99°36'11.1"	L-TiO_2	0.70400	7	0.51290	6	5.1
Metepec	**d-51**	6.65	19°14'51.4"	99°36'14.3"	L-TiO_2	0.70402	7	0.51289	4	4.8
Texontepec proximal	**d-42**	4.30	19°14'22.6"	99°24'43.7"	L-TiO_2	0.70423	8	0.51290	7	5.1
Texontepec distal	**d-47**	4.54	19°15'00.3"	99°27'36.3"	L-TiO_2	0.70414	7	0.51288	4	4.7
Pelagatos	**d-25**	9.24	19°06'00.0"	99°50'00.0"	L-TiO_2	0.70410	8	0.51285	5	4.1
Tenango	**d-54**	4.49	19°06'58.0"	99°36'40.3"	L-TiO_2	0.70377	8	0.51285	7	4.1
Tenango	**TEB**	4.33	19°06'41.9"	99°37'49.4"	L-TiO_2	0.70379	8	0.51283	5	3.7
Esperanza	**d-56**	4.32	19°06'44.9"	99°25'35.1"	L-TiO_2	0.70404	7	0.51288	7	4.8
Cuate Grande	**d-53**	8.51	19°11'27.2"	99°26'18.0"	Trans.	0.70365	7	0.51295	4	6.0
Capulhuac	**d-45**	8.59	19°11'50.0"	99°27'26.4"	Trans.	0.70363	7	0.51293	5	5.6
Tezoyuca	**d-37**	8.24	18°48'40.0"	99°12'36.0"	H-TiO_2	0.70396	7	0.51280	4	3.2
Tenango	**XTN**	9.93	19°05'22.4"	99°37'35.3"	Xenol.	0.70428	7	0.51277	5	2.5
Lama	**L2**	2.49	19°07'00.3"	99°33'15.6"	Xenol.	0.70391	7	0.51290	7	5.0

(H-TiO_2 series). Following Arai (1994) such Cr# variations should reflect the presence of important heterogeneities in the mantle source, suggesting the existence of a more depleted source for the L-TiO_2 with respect to the H-TiO_2 magmas. The unusual high TiO_2 concentrations found in SCVF rocks encouraged some authors to propose that SCVF magmas were not related to the subduction of the Cocos plate beneath Mexico. In fact, Márquez *et al.* (1999a, 1999b) and Márquez and De Ignacio (2002) proposed the upwelling of a deep-seated mantle plume in central Mexico capable of generating OIB-like magmas, whereas Verma (2000, 2002) proposed the presence of a passive rift and the generation of magma through decompression melting of an unmetasomatized mantle wedge. On the contrary, other authors reconciled the presence of SCVF enriched magmas through subduction of the Cocos slab causing the advection of enriched mantle portions from the back-arc mantle (Wallace and Carmichael, 1999), or the presence of a slab window able to induce a deep mantle flow into the wedge region (Ferrari, 2004).

By using the trace element and Sr-Nd isotopic data of the mafic products of western SCVF (Pelagatos and Tezoyuca cinder cones) some alternative considerations can be made to explain these chemical features of the mantle

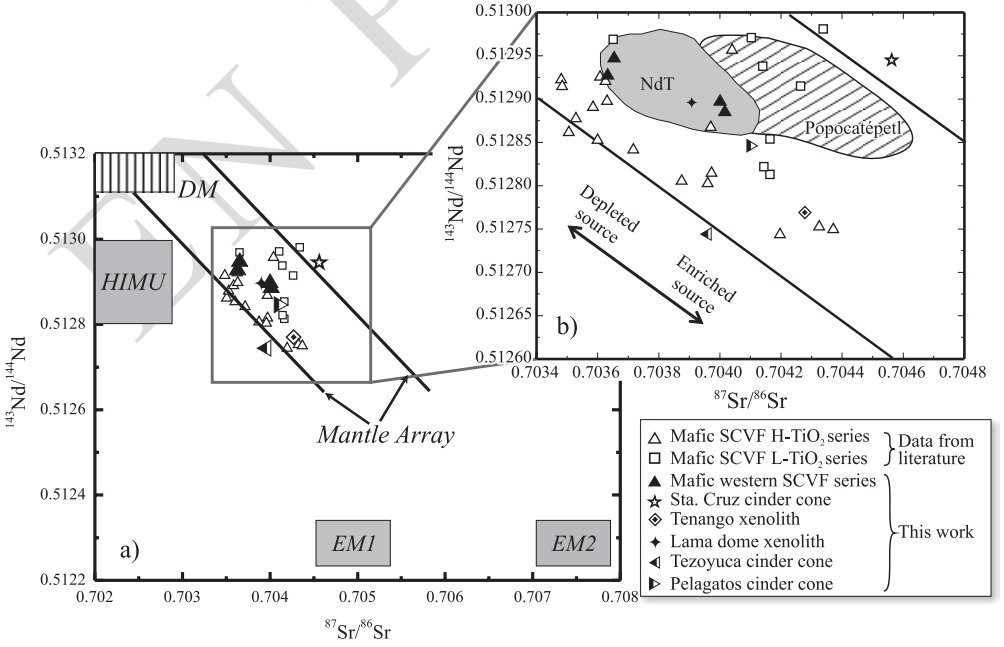

Figure 10. $^{143}Nd/^{144}Nd$ *vs*. $^{87}Sr/^{86}Sr$ for mafic volcanic rocks (MgO ≥6.0 wt.%), Sta Cruz cinder cone and crustal xenoliths of the Tenango area. a) DM: Depleted mantle; *EM1*: enriched mantle 1; *EM2*: enriched mantle 2, *HIMU*: high $^{238}U/^{204}Pb$ mantle; data from Zindler and Hart (1986). b) The gray-filled area represents the isotopic ratios of nearby Nevado de Toluca volcano (NdT), whereas the area filled with the line pattern represents data from Popocatépetl volcano. Data provenance: Verma (2000); Velasco-Tapia (2002); Martínez-Serrano *et al.*, 2004, Siebe *et al.* (2004b) and Schaaf *et al.* (2005).

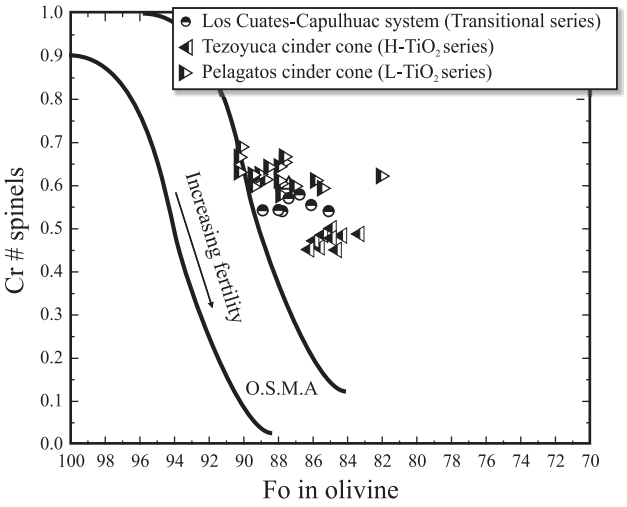

Figure 11. Cr# [100 Cr/(Cr+Al)] in spinel *vs*. Fo in olivine for Tezoyuca (H-TiO_2 series), Pelagatos (L-TiO_2 series), and Los Cuates-Capulhuac system (transitional series). Olivine Spinel Mantle Array (O.S.M.A.) is taken from Arai (1994). Notice the difference between the two main series represented by Tezoyuca and Pelagatos magmas. See text for more details.

source beneath Central Mexico. The multielement diagram of Figure 8a shows that the mafic L-TiO_2 and shoshonitic magmas from Sta. Cruz cinder cone are characterized by clear negative anomalies of HFSE such as Nb, Ta and Ti. These patterns suggest the occurrence of subduction-related metasomatic processes beneath SCVF, weakening the hypothesis of a rift-related magma genesis.

On the other hand, the hypothesis of a mantle plume to explain the OIB-like signature of SCVF rocks can be tested by using the trace element patterns and Sr-Nd isotopic ratios of H-TiO_2 products. Zindler and Hart (1986) concluded that the genesis of OIB magmas could be modeled by the interaction (*e.g.*, mixing) between variable amounts of a depleted mantle (DM; $^{143}Nd/^{144}Nd$ ~0.5132; $^{87}Sr/^{86}Sr$ ~0.702) and one (or more) end-members like a HIMU source (high μ, where μ = $^{238}U/^{204}Pb$), markedly enriched in U, Th and HFSE, or the Enriched Mantle (EM) characterized by low $^{143}Nd/^{144}Nd$ values (≤0.5124) and high $^{87}Sr/^{86}Sr$ values (~0.705 for EM1 and >0.707 for EM2 types) (Figure 10a). Although the lower values of $^{87}Sr/^{86}Sr$ of most mafic rocks belonging to the H-TiO_2 series could be taken as an evidence of HIMU component in the mantle source, several evidences argue against it. First of all, by comparing the incompatible elements of H-TiO_2 rocks (Tezoyuca cinder cone) with a typical HIMU magma as the Tubuai Island basalts (Chauvel *et al.*, 1992) (Figure 8c), dramatic differences are found in Th, U, K, Ta, Nb, La, Ce, and Pb contents. Moreover, Cervantes and Wallace (2003a) found high H_2O contents (~3.2 wt.%) in olivine glass inclusions of the H-TiO_2, high-Nb rocks of Tepetlapa (central SCVF; Figure 8c), characteristic absent in typical HIMU magmas (*e.g.*, Nadeau *et al.*, 1993; Dixon *et al.*, 2002; Workman *et al.*, 2006). Finally, although only few lead isotope data are available for the less evolved magmas of the SCVF, they show no differences between H-TiO_2 and L-TiO_2 series, and the values found ($^{206}Pb/^{204}Pb$=18.651–18.803; $^{207}Pb/^{204}Pb$= 15.570–15.643 and $^{208}Pb/^{204}Pb$=38.426–38.656) are far from those expected in HIMU end members ($^{206}Pb/^{204}Pb$ >21; $^{207}Pb/^{204}Pb$ >15.8 and $^{208}Pb/^{204}Pb$ >40.5, Chauvel *et al.*, 1992). Therefore, we argue against the occurrence of a HIMU contribution (*e.g.*, for mixing at mantle level) in the Mexican mantle wedge. On the other hand, the negligible variations of $^{143}Nd/^{144}Nd$ ratios of mafic rocks of the SCVF (Figure 10a) suggest that these magmas might not be linked neither to an EM component at their source. In short, the occurrence of a mantle plume below central Mexico is also poorly supported by the available data.

At this point, it seems more plausible that the genesis of SCVF magmas is linked to the subduction of the Cocos plate beneath Mexico. Therefore, any new model should be able to explain the different enrichments in TiO_2 and other HFSE found in the area. Although these elements are considered immobile in aqueous fluids arising from the slab (*e.g.*, Kogiso *et al.*, 1997), many authors suggest that water-rich silicate melts from the subducted sediments and/or slab, could be an efficient medium to transport such conservative elements into the mantle wedge (*e.g.*, Kepezhinskas *et al.*, 1997; Walker *et al.*, 2001; Green, 2005). In this context, the downward warping of the Cocos plate beneath central Mexico inferred by Pardo and Suárez (1995) and Manea *et al.* (2004) could induce a rapid heating of the slab, leading to important consequences for magma genesis in central Mexico. In particular, phase relations studies of Pawley and Holloway (1993) and Kessel *et al.* (2005) indicate that at high temperature, an eclogitic slab could generate fluxes of H_2O-SiO_2 bearing fluids/melts able to transport high contents of incompatible elements such as LILE or HFSE through the mantle wedge. These fluids/melts are not only able to induce partial melting of the mantle peridotite, but may hydrate it with the consequent fractionation of mineral phases such as amphibole and/or micas as disseminated crystals or in centimeter- to meter-thick veins (Tatsumi, 1989; Arculus, 1994). Chemical data of amphibole-bearing xenoliths as well as experimental data (Brenan *et al.*, 1995; Ionov and Hofmann, 1995; Tiepolo *et al.*, 2000; 2001) demonstrated that calcic amphiboles such as kaersutite or pargasite as well as phlogopite, may crystallize in mantle conditions and host notable concentrations of LILE and HFSE otherwise highly incompatible in the anhydrous mantle mineralogy. Subsequently, partial melting of such hydrated peridotite could produce low density melts enriched in incompatible elements such as HFSE, REE and alkalis that resemble in composition the OIB and rift-related magmas (Menzies *et al.*, 1987). In this context, the mantle xenoliths described by Blatter and Carmichael (1998b) and Mukasa *et al.* (2007) hosted in the nearby Quaternary products of Valle de Bravo (~60 km west of studied area) are of noteworthy interest. Overall, the heterogeneous mineral assemblage of olivine + pyroxenes + spinel and Cr-pargasite confirms that a hydrous

mantle wedge is present beneath central Mexico.

As shown in Figure 12a, 5–15% partial melting of a mantle source constituted by 37% olivine + 40% orthopyroxene + 16% clinopyroxene + 4% spinel + 3% of amphibole (kaersutite in our model), compositionally similar to the xenoliths X-30 and X-33 of Mukasa *et al.* (2007), is able to generate melts with steep REE patterns as those observed in the H-TiO_2 mafic magmas. To obtain the less fractionated pattern of the L-TiO_2 mafic magmas, the model needs lower degrees of partial melting (1-5%) of a depleted mantle similar to that proposed by Mukasa *et al.* (2007) and constituted by 33% olivine + 45% orthopyroxene + 19% clinopyroxene + 3% spinel (Figure 12b). However, this doesn't imply that hybrid mantle source portions could not exist beneath the SCVF. In fact, by using the two end-members mixing formula of Bryan *et al.* (1969) it was possible to reproduce most of the hygromagmatophile element contents found in the L-TiO_2, H-TiO_2 and transitional series of the mafic magmas SCVF (Figure 13). The existence of a hybrid mantle source is also supported by the differences found in spinel composition (Figure 11), and bulk rock analyses (Figure 6).

The genesis of Sta. Cruz magmas merits careful attention because of its special composition: an extremely high LILE/HFSE ratio with respect to nearby lavas (*e.g.*, $(Ba/Nb)_N$ ~10 times higher than samples from Los Cuates-Capulhuac complex), enrichment in K_2O, light REE, P_2O_5 and other incompatible trace elements, and high $^{87}Sr/^{86}Sr$ ratio. These characteristics suggest a stronger contribution of fluids or melts from the altered slab (*e.g.*, De Paolo and Wasserburg, 1977). The chemical composition of Sta. Cruz rocks is similar to the lamprophyric magmas described by

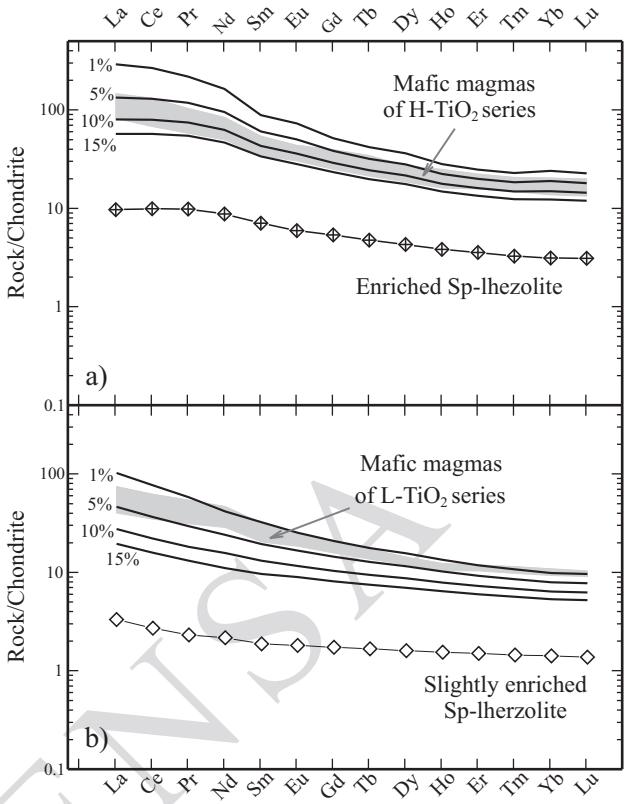

Figure 12. Calculated REE patterns for partial melting of different mantle sources. Degrees of partial melting between 5 and 15% of an enriched Sp-lherzolite can generate the compositional ranges shown by the mafic magmas of the H-TiO_2 series. Instead, lower degrees of partial melting (1–5 %) of a more depleted source are needed to create the REE patterns of the mafic L-TiO_2 magmas. Partition coefficient values were taken from McKenzie and O'Nions (1991), Fujimaki *et al.* (1984), and Bottazzi *et al.* (1999).

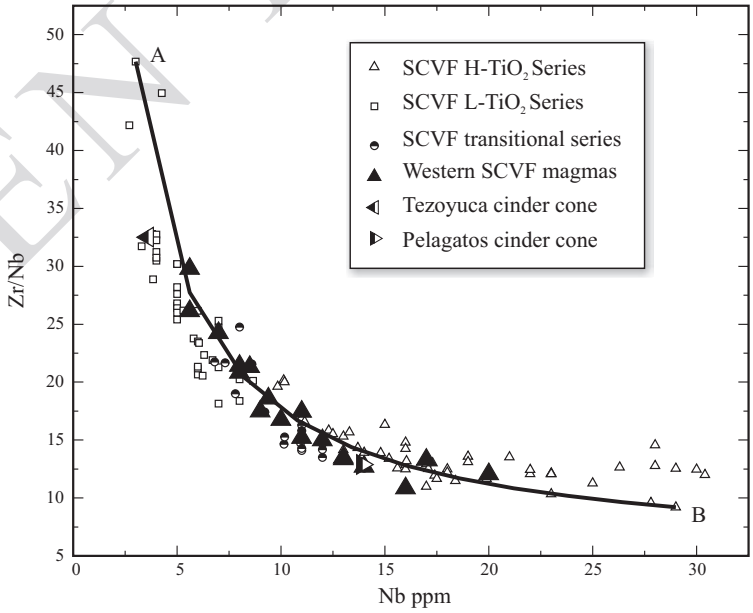

Figure 13. Nb (ppm) *vs*. Zr/Nb of SCVF mafic magmas. Black line represents the mixing line between L-TiO_2 end-member A (sample 232 of Wallace and Carmichael, 1999) and H-TiO_2 end-member B (sample MXC-14 of Nixon 1988) traced following Bryan *et al.* (1969). The very good fitting of the mixing line suggests the existence of a hybrid mantle source beneath SCVF.

Luhr (1997) and Luhr *et al.* (1989) in western Mexico, which were interpreted as being formed by partial melting in the mantle wedge of phlogopite-bearing veins, generated by the interaction of hydrous melts with the peridotitic wall rock.

Magmatic evolution

The eruptive centers of the SVCF are scattered over an area of ~2,400 km^2. Each vent represents a different magmatic source undergoing unique differentiation processes at crustal levels. Notwithstanding these considerations, a general crystallization history can be depicted by using the chemical composition and the isotopic ratios of the studied rocks.

Because the H-TiO_2 and L-TiO_2 series of the SCVF may be generated by different contributions from the slab, and because H_2O has significant effects during mantle melting processes influencing the SiO_2 contents of the mantle derived magmas (*e.g.*, Kushiro, 1972; 1990; Hirose, 1997; Gaetani and Grove, 2003; Parman and Grove, 2004), MgO was chosen as differentiation index in most chemical variation diagrams of Figures 14 and 15. Although MgO contents of L- and H-TiO_2 series of SCVF are comparable, the former series shows lower values of TiO_2, alkalis, and HFSE, whereas it appears slightly enriched in SiO_2, Al_2O_3/CaO and compatible elements such as Cr. On the other hand, the two series do not present significant differences in LILE concentrations (not shown).

In order to test the fractional crystallization process of the western SCVF magmas, we used the thermodynamic model MELTS of Ghiorso and Sack (1995) for major element composition. Samples Mx40 (H-TiO_2 series) and d-25 (L-TiO_2 series) were proposed as mafic end-members (Table A6, Figure 14a). By fixing the crystallization pressure between 8 and 1.5 kbar with H_2O contents of 3.5–5 wt.%, MELTS suggests the occurrence of olivine (Fo_{86}) + spinel as near liquidus phases at temperatures of 1,200–1,250 °C. Proceeding with the magmatic evolution at MgO contents of 4.5–5 wt.%, clinopyroxene (Di_{53}) appears in the melt, while olivine is progressively substituted by orthopyroxene (En_{90}). Labradoritic plagioclase and ilmenite appear later, at MgO concentrations of 4 wt.% or less. The good correlation between the MELTS calculation and the compositions of the mineral phases found in thin section, supports the fact that crystal fractionation is the main process occurring in western SCVF magmas. Moreover, MELTS calculates successfully several variations in the major element concentrations observed in the western Sierra Chichinautzin rocks (Figure

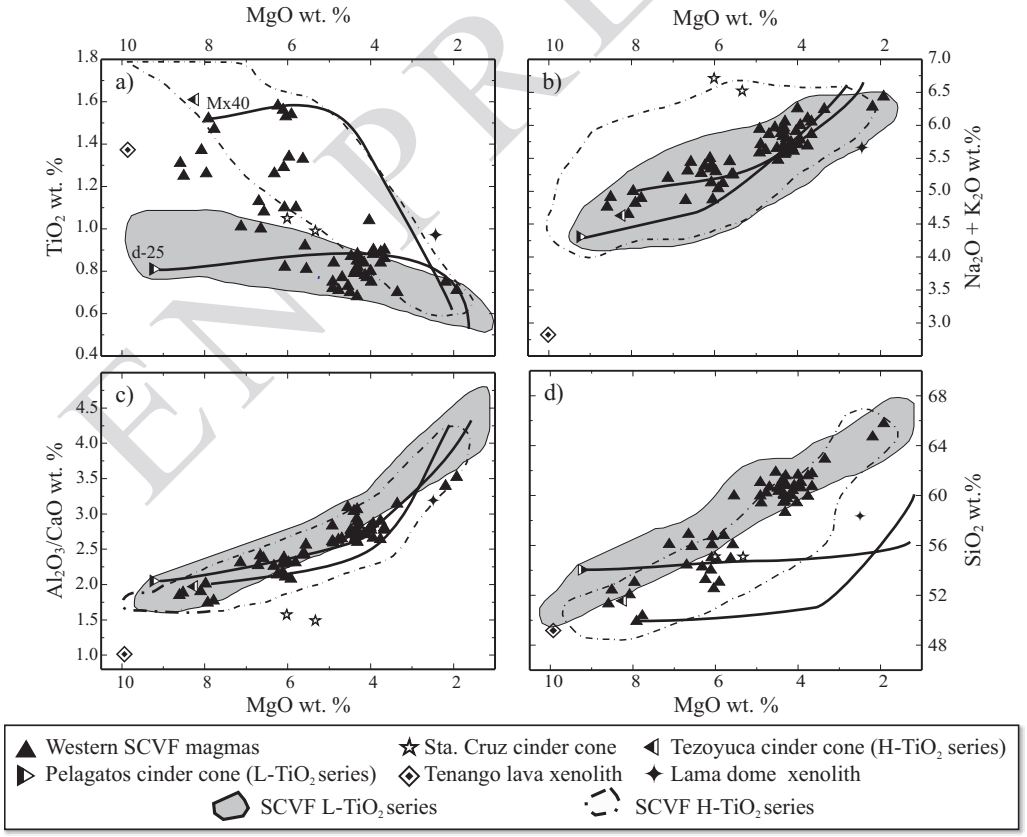

Figure 14. Representative major element variation diagrams of SCVF magmas. Thick lines represent the composition of residual liquids calculated by the MELTS algorithm (Ghiorso and Sack, 1995) by using olivine + Ti-Magnetite (for H-TiO_2 magmas only) + pyroxene ± plagioclase. A good fit between the calculated line of descent and the plotted data is observed for TiO_2, alkalis and Al_2O_3/CaO, but not for SiO_2.

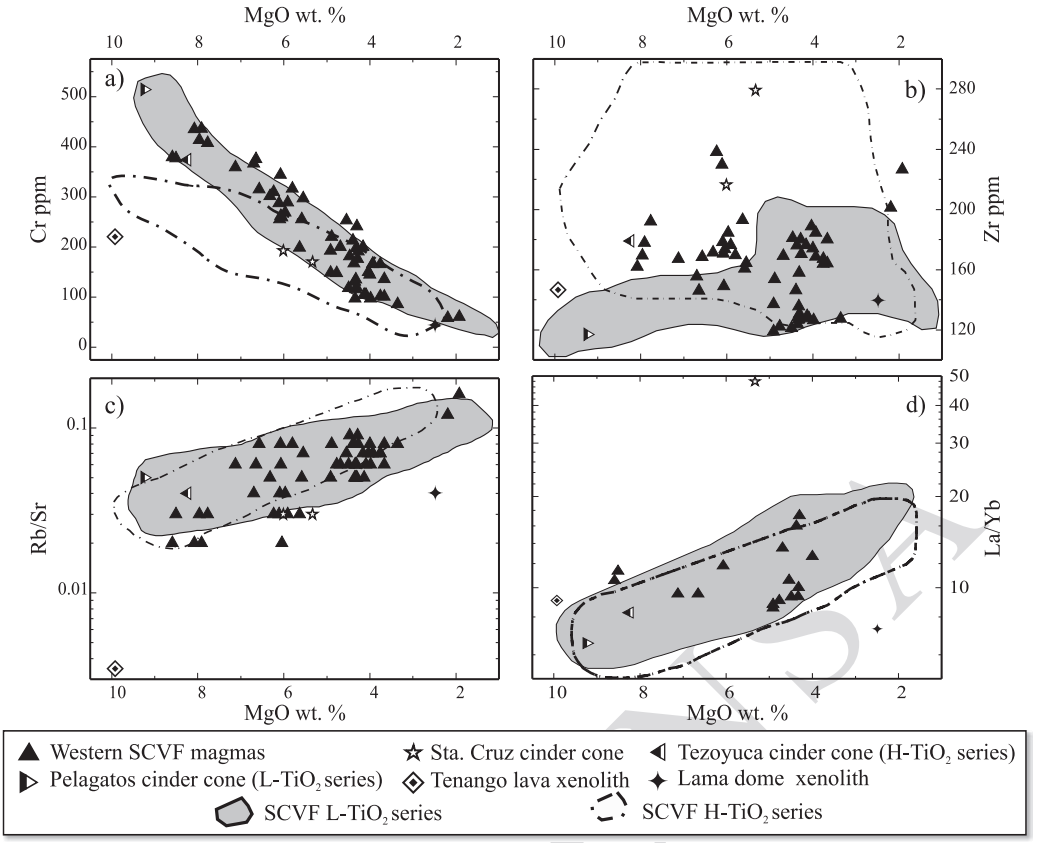

Figure 15. Representative trace element variation diagrams of SCVF magmas.

14a-c). In particular, the occurrence of Ti-magnetite at high temperature is able to drop the TiO_2 contents of the liquid from 1.52 wt.% to less than 1 wt.% after a fractionation of 7–8 wt.% of this mineral. One exception is represented by the quasi-compatible behavior shown by Zr in some mafic magmas, because its low partition coefficient values should produce an opposite trend. Nevertheless, the experimental work of Nielsen *et al.* (1994) indicate that the partition coefficients of Zr and other HFSE are far from being constant in magmatic systems and are probably correlated with the partition coefficients of Ti reaching values of >2 in Ti-magnetite. Therefore, the presence of Ti-bearing opaque phases during the early stages of crystallization could explain the compatible behavior of Ti and Zr.

However, the analyzed rocks show compositional characteristics that are difficult to explain with the occurrence of fractional crystallization as the sole mechanism. In particular, the SiO_2 increment is steeper with respect to values calculated by the MELTS algorithm (Figure 14d) and the fractionation of Ol + Px ± Ox ± Plg does not seem to be capable of varying significantly the ratios of incompatible elements such as Rb/Sr or La/Yb (Figure 15c-d).

Although high magma supply rates from the mantle can produce well-sustained conduits that would avoid important contributions of surrounding crustal rocks (*e.g.*, Hansen and Nielsen, 1999), the inverse correlation between $^{87}Sr/^{86}Sr$ ratios and MgO suggests crustal contributions during the evolution of the Sierra Chichinautzin magmas (Figure 16). On the other hand, Figures 14, 15 and 16 indicate that the crustal xenoliths found in Tenango lava and Lama dome are not suitable candidates for contaminant of

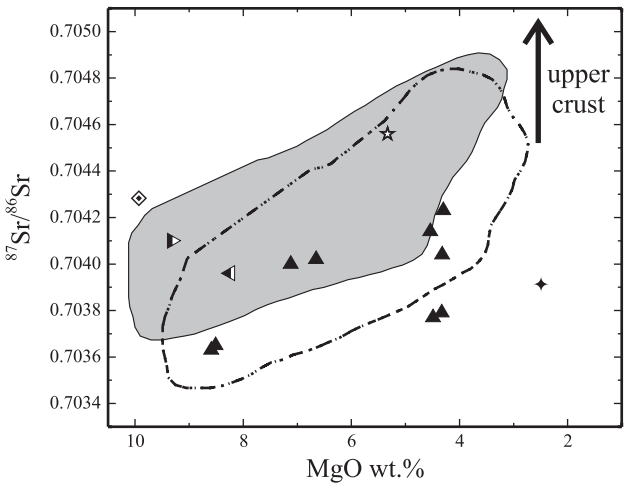

Figure 16. MgO (wt.%) *vs*. $^{87}Sr/^{86}Sr$ diagram for SCVF magmas. The increase of $^{87}Sr/^{86}Sr$ ratio with magmatic evolution suggests the occurrence of crustal contamination along with crystal fractionation. Symbols as in Figure 15.

the western Sierra Chichinautzin magmas because of their low Rb contents, and LREE/HREE and $^{87}Sr/^{86}Sr$ ratios.

Verma (1999) suggested that high grade partial melting (~50%) of a granulitic lower crust would be able to generate magmas with isotopic and REE compositions broadly similar to the dacitic rocks of the Sierra Chichinuatzin. However, lower crustal material is characterized by low concentrations of Rb (<30 ppm), Th (<5 ppm), La (<11 ppm) and low values of Th/Yb (<2), Rb/Sr (<0.1), Rb/Ba (<0.1), La/Yb (0.1) and Nd/Sm (<4) (*e.g.*, Taylor and McLennan, 1985; Schaaf *et al.*, 1994). Therefore, the higher values shown by the Sierra Chichinautzin magmas point to an upper, instead of a lower, crustal end-member (*e.g.*, Figure 17). Nevertheless, one more thing need to be addressed: What kind of crust is required to generate only small changes in REE concentration as well as in $^{87}Sr/^{86}Sr$ values during the magmatic evolution (Figures 16, 17 and 18)? Although the nature of the crust beneath the Sierra Chichinautzin is poorly constrained, and therefore more exhaustive studies are needed, the granodioritic xenoliths found by Schaaf *et al.* (2005) in the nearby Popocatépetl volcano deposits, fulfill many of these requirements and consequently may represent possible contaminants of ascending magmas in central Mexico (Figure 18).

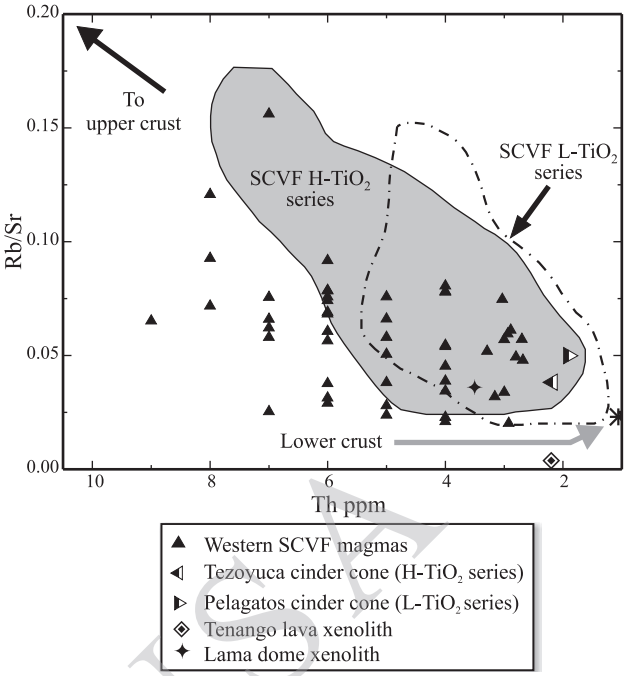

Figure 17. The increase of Rb/Sr and Th with magmatic evolution of the western SCVF magmas suggests magma contamination with upper crustal rather than with lower crustal material. Values of the upper and lower crust from Taylor and McLennan (1985).

CONCLUSIONS

The Quaternary mafic magmatism of SCVF is characterized by important heterogeneities, such as the variable HFSE enrichments, that triggered the debate on the role of the subducting slab in the magma genesis of the entire Trans-Mexican Volcanic Belt and arc volcanism in general. In fact, although the L-TiO_2 series and the high K_2O rocks (Sta. Cruz cinder cone) are easily interpreted with a classical subduction model (*e.g.*, Gill, 1981), the presence of mafic H-TiO_2 magmas would not fit the models for such a geodynamic setting. However, recent experimental data on the behavior of HFSE in hydrated mantle paragenesis reconciled such HFSE enriched compositions with magma generation processes in convergent margins. Hence, partial melting of a heterogeneous amphibole-bearing mantle seems to explain the whole rock composition range observed in the western SCVF. Finally, chemical and isotopic data suggest that fractional crystallization and crustal contamination are the main evolution processes in the studied area.

ACKNOWLEDGEMENTS

The authors wish to thank John Eichelberger, Peter Schaaf, Yuri Taran, Christopher Nye and Simon Hughes for stirring and focusing discussions; Gabriela Solís, Luisa Guarnieri, Riccardo Avanzinelli, and Elena Boari for their help during isotope analysis; Gloria Vaggelli and Filippo Olmi (†) for allowing access to microprobe facilities; Lilia Arana for the field work, and S. Verma for the valuable and insightful comments, as well as editorial handling. The reviews by A. Márquez and P. Wallace helped substantially to clear up ideas of this manuscript. This work is part of the Master Thesis of the senior author, which was partly supported by CNR bilateral grant (bando # 203.05.23) issued to

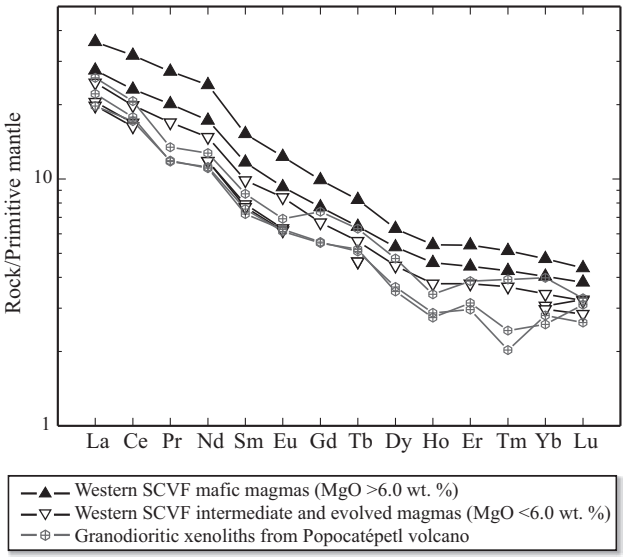

Figure 18. Rare Earth Elements diagram of mafic and evolved rocks of the Tenango area plus granodiritic xenoliths from Popocatépetl volcano (Schaaf *et al.*, 2005). Normalization follows primitive mantle values of Sun and McDonough (1989).

Lorenzo Meriggi. This work was supported by CONACYT grant 47226 to J.L. Macías.

APPENDIX A. SUPPLEMENTARY DATA

Tables A1-A6 can be found at the journal web site <http://satori.geociencias.unam.mx/>, in the table of contents of this issue (electronic supplement 25-2-01) .

REFERENCES

Albee, A.L., Ray, L., 1970, Correction factors for electron probe analysis of silicate, oxides, carbonates, phosphates and sulphates: Analytical Chemistry 42, 1408–1414.

Arai, S., 1994, Compositional variation of olivine–chromian spinel in Mg-rich magmas as a guide to their residual spinel peridotites: Journal of Volcanology and Geothermal Research, 59, 279–293.

Arce, J.L., Macías, J.L., Vázquez-Selem, L., 2003, The 10.5 ka Plinian eruption of Nevado de Toluca Volcano, Mexico. Stratigraphy and hazard implications: Geological Society of America Bulletin, 115, 230-248.

Arculus, R.J., 1994, Aspects of magma genesis in arcs: Lithos, 33, 189-208.

Arculus, R.J., 2003, Use and abuse of the Terms Calcalkaline and Calcalkalic: Journal of Petrology, 44, 929-935.

Avanzinelli, R., Boari, E., Conticelli, S., Francalanci, L., Guarnieri, L., Perini, G., Petrone, C.M., Tommasini, S., Ulivi, M., 2005, High precision Sr, Nd, and Pb isotopic analyses and reproducibility using new generation Thermal Ionization Mass Spectrometer: aims and perspective for Isotope Geology Applications: Periodico di Mineralogia, 74, 147-166.

Bence, A.E., Albee, A.L., 1968, Empirical correction factors for electron microanalysis of silicates, oxides, carbonates, phosphates and sulphates: Journal of Geology, 76, 382-403.

Blatter, D.L., Carmichael, I.S.E., 1998a, Plagioclase-free andesite from Zitácuaro (Michoacán), Mexico: petrology and experimental constraints: Contributions to Mineralogy and Petrology, 132, 121-138.

Blatter, D.L., Carmichael, I.S.E., 1998b, Hornblende peridotite xenoliths from central Mexico reveal the highly oxidized nature of subarc upper mantle: Geology 26, 1035–1038.

Blatter, D.L., Carmichael, I.S.E., 2001, Hydrous phase equilibria of a Mexican high-silica andesite: A candidate for a mantle origin?: Geochimica et Cosmochimica Acta, 65, 4043–4065.

Bloomfield, K., 1974, The age and significance of the Tenango Basalt, central Mexico: Bulletin of Volcanology, 37, 586-595.

Bloomfield, K., 1975, A late Quaternary volcano field in central Mexico: Geologische Rundschau, 64, 476- 497.

Bottazzi, P., Tiepolo, M., Vannucci, R., Zanetti, A., Brumm, R., Foley, S.F., Oberti, R., 1999, Distinct site preference for heavy and light REE in amphibole and the prediction of $^{Amph/L}D_{REE}$: Contributions to Mineralogy and Petrology, 137, 36-45.

Brenan, J.M., Shaw, H.F., Ryerson, F.J., Phinney, D.L., 1995, Experimental determination of trace-element partitioning between pargasite and synthetic hydrous andesitic melt: Earth and Planetary Science Letters, 135, 1-11.

Bryan, W.B., Finger, L.W., Chayes, F., 1969, Estimating proportions in petrographic mixing equations by least-squares approximation: Science, 163, 926-927.

Carmichael, I.S.E., Lange, R.A., Luhr, J.F., 1996, Quaternary minettes and associated volcanic rocks of Mascota, Western Mexico: a consequence of plate extension above a subduction modified mantle wedge: Contributions to Mineralogy and Petrology, 124, 302-333.

Castillo, R.P., Janney, P.E., Solidum, R.U., 1999, Petrology and geochemistry of Camiguin Island, southern Philippines: insight to the source of adakites and other lavas in a complex arc setting: Contributions to Mineralogy and Petrology, 134, 33-51.

Cervantes P., Wallace P.J., 2003a, Role of H_2O in subduction-zone magmatism: New insight from melt inclusions in high-Mg basalts from central Mexico: Geology, 31, 235-238.

Cervantes, P., Wallace, P., 2003b, Magma degassing and basaltic eruption styles: a case of ~2000 year BP Xitle volcano in central Mexico: Journal of Volcanology and Geothermal Research, 120, 249-270.

Chauvel, C., Hofmann, A.W., Vidal, P., 1992, HIMU-EM: The French Polynesian connection: Earth and Planetary Science Letters, 110, 99-119.

Conticelli, S., 1998, Effects of crustal contamination on ultrapotassic magmas with lamproitic affinity: mineralogical, geochemical and isotope data from the Torre Alfina lavas and xenoliths, Central Italy: Chemical Geology, 149, 51-81.

Conticelli, S., Peccerillo, A., 1992, Petrology and geochemistry of potassic and ultrapotassic volcanism in central Italy: petrogenesis and inferences on the evolution of the mantle sources: Lithos, 28, 221–240.

Conticelli, S., Francalanci, L., Manetti, P., Cioni, R., Sbrana, A., 1997, Petrology and geochemistry of the ultrapotassic rocks from the Sabatini Volcanic District, Central Italy: the role of evolutionary processes in the genesis of variably enriched alkaline magmas: Journal of Volcanology and Geothermal Research, 75, 107-136.

Conticelli, S., D'Antonio, M., Pinarelli, L., Civetta L., 2002, Source contamination and mantle heterogeneity in the genesis of Italian potassic and ultrapotassic volcanic rocks: Sr-Nd-Pb isotope data from Roman Province and Southern Tuscany: Mineralogy and Petrology, 74, 189-222.

Conticelli, S., Carlson, R.W., Window, E., Serri, G., 2007, Chemical and isotopic composition (Os, Pb, Nd, and Sr) of Neogene to Quaternary calc-alkalic, shoshonitic and ultrapotassic mafic rocks from the Italian Peninsula: inferences on the nature of their mantle source: Geological Society of America, Special Paper, 418, 171-202.

De Cserna, Z., Fries, C., Rincón-Orta, C., Silver, L.T., Westley, H., Solorio-Munguia, J., Schmitter-Villava, E., 1974, Datos geocronométricos terciarios de los Estados de México y Guerrero: Boletín Asociación Mexicana de Geólogos Petroleros, 26, 263-273.

DePaolo, D.J., Wasserburg, G.J., 1977, The source of Island arcs as indicated by Nd and Sr isotopic studies: Geophysical Research Letters, 4, 465-468.

Defant, M.J., Drummond, M.S., 1990, Derivation of some modern arc magmas by melting of young subducted lithosphere: Nature, 347, 662-665.

Dixon, J.E., Leist, L., Langmuir, C., Schilling, J.-G., 2002, Recycled dehydrated lithosphere observed in plume-influenced mid-ocean-ridge-basalt: Nature, 420, 385-389.

Drummond, M.S., Defant, M.J., 1990, A model for trondhjemite-tonalite-dacite genesis and crustal growth via slab melting: archean to modern comparisons: Journal of Geophysical Research, 95, 21503–21521.

Elliott, T.R., Plank, T., Zindler, A., White, W.M., Bourdon, B., 1997, Element transport from slab to volcanic front in the Mariana arc: Journal of Geophysical Research, 102, 14991– 15019.

Feigenson, M.D., Carr, M.J., 1993, The source of central American lavas: inferences from geochemical inverse modeling: Contributions to Mineralogy and Petrology, 113, 226-235.

Ferrari, L., 2004, Slab detachment control on mafic volcanic pulse and mantle heterogeneity in central Mexico: Geology, 32, 77–80.

Ferrari, L., Conticelli, S., Vaggelli, G., Petrone, C. M., Manetti, P., 2000, Late Miocene volcanism and intra-arc tectonics during the early development of the Trans-Mexican Volcanic Belt: Tectonophysics, 318, 161–185.

Ferrari, L., Petrone, C. M., Francalanci, L., 2001, Generation of oceanic-island basalt–type volcanism in the western Trans-Mexican volcanic belt by slab rollback, asthenosphere infiltration, and variable flux melting: Geology, 29, 507–510.

Francalanci, L., Taylor, S.R., McCulloch, M.T., Woodhead, J.D., 1993, Geochemical and isotopic variations in the calc-alkaline rocks of Aeolian arc, southern Tyrrhenian Sea, Italy: constraints on magma genesis: Contributions to Mineralogy and Petrology, 113, 300-313.

Francalanci, L., Tommasini, S., Conticelli, S., Davies, G.H., 1999, Sr isotope evidence for short magma residence time for the 20th century activity at Stromboli volcano, Italy: Earth and Planetary Science Letters, 167, 61-69.

Francalanci, L., Tommasini, S., Conticelli, S., 2004, The volcanic activity of Stromboli in the 1906-1998 AD period: mineralogical, geochemical and isotope data relevant to the understanding of Strombolian activity: Journal of Volcanology and Geothermal Research, 131, 179-211.

Franzini, M., Leoni, L., Saitta, M., 1972, A simple method to evaluate the matrix effect in X-ray fluorescence analysis: X-ray Spectrometry, 1, 151-154.

Frey, F.A., Green, D.H., Roy, S.D., 1978, Integrated model of basalt petrogenesis: a study of quartz tholeiites to olivine melilitites from South Eastern Australia, utilizing geochemical and experimental data: Journal of Petrology, 19, 463– 513.

Fujimaki, H., Tatsumoto, M., Aoki, K., 1984, Partition coefficients of Hf, Zr, and REE between phenocrysts and groundmass: Journal of Geophysical Research, 89, 662-672.

Gaetani, G.A., Grove, T.L., 2003, Experimental constraints on melt generation in the mantle wedge, *in* Eiler, J. (ed), Inside the Subduction Factory: American Geophysical Union, Geophysical Monograph Series, 138, 107-134.

García-Palomo, A., Macías, J.L., Garduño, V.H., 2000, Miocene to Recent structural evolution of the Nevado de Toluca volcano region, central Mexico: Tectonophysics, 318, 281–302.

García-Palomo, A., Macías, J.L., Arce, J.L., Capra, L., Garduño, V.H., Espíndola, J.M., 2002a, Geology of Nevado de Toluca Volcano and surrounding areas, Central Mexico: Geological Society of America, Map and Chart Series, MCH089.

García-Palomo, A., Macías, J.L., Tolson, G., Valdéz, G., Mora, J.C., 2002b, Volcanic stratigraphy and geological evolution of the Apan region, east-central sector of the Trans-Mexican Volcanic Belt: Geofísica Internacional, 41, 133-150.

Ghiorso, M.S., Sack R.O., 1995, Chemical mass transfer in magmatic processes IV. A Revised and internally consistent thermodynamic model for the interpolation and extrapolation of liquid-solid equilibria in magmatic systems at elevated temperature and pressure: Contributions to Mineralogy and Petrology, 119, 197-212.

Gill, J.B., 1981, Orogenic and plate tectonics: Berlin, Springer-Verlag, 390 p.

Gómez-Tuena, A., Langmuir, C.H., Goldstein, S.L., Straub, S.M., Ortega-Gutiérrez, F., 2007, Geochemical Evidence for Slab Melting in the Trans-Mexican Volcanic Belt: Journal of Petrology, 48, 537-562.

Green, D.H., 1971, Composition of basaltic magmas as indicators of origin: application to oceanic volcanism: Philosophical Transactions of the Royal Society of London, Series A268, 707-725.

Green, N.L., 2005, Influence of slab structure on basalt source regions and melting conditions: REE and HFSE constraints from the Garibaldi volcanic belt, northen Cascadia subduction system: Lithos, 87, 23-49.

Hansen, H., Nielsen, T.F.D., 1999, Crustal contamination in Palaeogene East Greenland flodd basalts: plumbing system evolution during continental rifting: Chemical Geology, 157, 89-118.

Hasenaka, T., Carmichael I.S.E., 1985, The cinder cones of Michoacán-Guanajuato, central Mexico: their age, volume and distribution, and magma discharge rate: Journal of Volcanology and Geothermal Research, 25, 105-124.

Hirose, K., 1997, Melting experiments on lherzolite KLB-1 under hydrous conditions and generation of high-magnesian andesitic melts: Geology, 25, 42–44.

Hofmann, A.W., 1988, Chemical differentiation of the Earth: the relationship between mantle, continental crust, and oceanic crust: Earth and Planetary Science Letters, 90, 297-314.

Ionov, D.A., Hofmann, A.W., 1995. Nb-Ta-rich mantle amphiboles and micas: Implications for subduction-related metasomatic trace element fractionation: Earth and Planetary Science Letters, 131, 341-356.

Irvine, T.N., Baragar, W.R.A., 1971, A guide to the chemical classification of the common rocks: Canadian Journal of Earth Science, 8, 523-548.

Kessel, R., Schmidt, M.W., Ulmer, P., Pettke, T., 2005, Trace element signature of subduction-zone fluids, melts and supercritical liquids at 120-180 km depth: Nature, 437, 724-727.

Kepezhinskas, P., McDermott, F., Defant, M.J., Hochstaedter, A., Drummond, M.S., Hawkesworth, C.J., Koloskov, A., Maury R.C., Bellon H., 1997, Trace element and Sr-Nd-Pb isotopic constraints on a three-component model of Kamchatka Arc petrogenesis: Geochimica et Cosmochimica Acta, 3, 577-600.

Kogiso, T., Tatsumi, Y., Nakano, S., 1997, Trace element transport during dehydration processes in the subducted oceanic crust. 1. Experiments and implications for the origin of ocean island basalts: Earth and Planetary Science Letters, 148, 193-205.

Kushiro, I., 1972, Effect of H_2O on the composition of magmas formed at high pressures: Journal of Petrology, 13, 311–334.

Kushiro, I., 1990, Partial melting of mantle wedge and evolution of island arc crust: Journal of Geophysical Research, 95, 15929–15939.

Le Bas, M.J., Le Maitre, R.W., Streckeisen, A., Zanettin B., 1986, A chemical classification of volcanic rocks based on the total alkali-silica diagram: Journal of Petrology, 27, 745-750.

Luhr, J.F., 1997, Extensional tectonics and the diverse primitive volcanic rocks in the Western Mexican Volcanic Belt: The Canadian Mineralogist, 35, 473–500.

Luhr, J.F., Carmichael, I.S.E., 1981, The Colima Volcanic Complex: II. Late Quaternary cinder cones: Contributions to Mineralogy and Petrology, 76, 127-147.

Luhr, J.F., Carmichael, I.S.E., 1985, Jorullo Volcano, Michoacán, Mexico (1759-1774): the earliest stage of fractionation in calc-alkaline magmas: Contributions to Mineralogy and Petrology, 90, 142-161.

Luhr, J.F., Allan, J., Carmichael, I., Nelson, S., Hasenaka, T., 1989, Primitive calc-alkaline and alkaline rock types from the western Mexican volcanic belt: Journal of Geophysical Research, 94(B4), 4515-4530.

MacDonald, G.A., Katsura, T., 1964, Chemical compositions of Hawaiian lavas: Journal of Petrology, 5, 82-133.

Manea, V.C., Manea, M., Kostoglodov, V., Currie, C.A., Sewell, G., 2004, Thermal structure, coupling and metamorphism in the Mexican subduction zone beneath Guerrero: Geophysical Journal International, 158, 775-784.

Márquez, A., De Ignacio, C., 2002, Mineralogical and geochemical constraints for the origin and evolution of magmas in Sierra Chichinautzin, Central Mexican Volcanic Belt: Lithos, 62, 35–62.

Márquez, A., Oyarzun, R., Doblas, M., Verma, S.P., 1999a, Alkalic (ocean-island basalt type) and calc-alkalic volcanism in the Mexican volcanic belt: A case for plume-related magmatism and propagating rifting at an active margin?: Geology, 27, 51–54.

Márquez, A., Verma, S.P., Anguita, F., Oyarzun, R., Brandle, J.L., 1999b, Tectonics and volcanism of Sierra Chichinautzin: extension at the front of the Central Trans-Mexican Volcanic Belt: Journal of Volcanology and Geothermal Research, 93, 125–150.

Martín-del Pozzo, A.L., 1982, Monogenetic volcanism in sierra Chichinautzin, Mexico: Bulletin of Volcanology, 45, 9-24.

Martínez-Serrano, R.G., Schaaf, P., Solís-Pichardo, G., Hernández-Bernal, M.S., Hernández-Treviño, T., Morales-Contreras, J.J., Macías, J.L., 2004, Sr, Nd and Pb isotope and geochemical data from the Quaternary Nevado de Toluca volcano, a source of recent adakitic magmatism, and the Tenango Volcanic Field, Mexico: Journal of Volcanology and Geothermal Research, 138, 77-110.

McKenzie, D., O'Nions, R.K., 1991, Partial melt distribution from inversion of rare Earth element concentrations: Journal of Petrology, 32, 1021-1091.

Menzies, M., Rogers, N., Tindle, A., Hawkesworth, 1987, Metasomatic

and enrichment processes in lithospheric peridotites, and effect of Astenosphere-Lithosphere interaction, *in* Menzies, M.A., Hawkesworth, C.J. (eds.), Mantle Metasomatism: London, Academic Press, 472 p.

Meriggi, L., 1999, Studio petrologico e vulcanologico del vulcanismo monogenetico e fissurale dell'area di Toluca, México: Università degli Studi di Firenze Italy, Master Thesis, 113 p.

Morimoto, N., 1989, Nomenclature of pyroxenes: The Canadian Mineralogist, 27, 143–156.

Mukasa S.B., Blatter D.L., Andronikov A.V., 2007, Mantle peridotite xenoliths in andesite lava at El Peñon, central Mexican Volcanic Belt: Isotopic and trace element evidence for melting and metasomatism in the mantle wedge beneath arc: Earth and Planetary Science Letters, 260, 37-55.

Nadeau S., Philippot P., Pineau, F., 1993, Fluid inclusion and mineral isotopic composition (H-C-O) in eclogitic rocks as tracers of local fluid migration during high-pressure metamorphism: Earth and Planetary Science Letters, 114, 431-488.

Nelson, S.A., González-Caver, E., 1992. Geology and K–Ar dating of the Tuxtla volcanic field, Veracruz, Mexico: Bulletin of Volcanology, 1151, 85– 96.

Nicholls, I.A., Ringwood, A.E, 1973, Effect of water on olivine stability in tholeiites and the production of silica-saturated magmas in the island-arc environment: Journal of Geology, 81, 285-300.

Nielsen, R.L., Forsythe L.M., Gallahen W.E., Fisk M.R., 1994, Major- and trace-element magnetite-melt equilibria: Chemical Geology, 177, 167-191.

Nixon, G.T., 1988, Petrology of the younger andesites and dacites of Iztaccíhuatl volcano, Mexico: II. Chemical stratigraphy, magma mixing, and the composition ob basaltic magma influx: Journal of Petrology, 29, 265-303.

Osete, M.L., Ruíz-Martínez, V.C., Caballero, C., Galindo, C., Urrutia-Fucugauchi, J., Tarling, D.H., 2000, Southward migration of continental volcanic activity in the Sierra de Las Cruces, Mexico: palaeomagnetic and radiometric evidence: Tectonophysics, 318, 201–215.

Pardo, M., Suárez, G., 1995, Shape of subducted Rivera and Cocos plate in southern Mexico: seismic and tectonic implications: Journal of Geophysical Research, 100, 12357-12373.

Parman, S.W., Grove, T.L., 2004, Harzburgite melting with and without H_2O: Experimental data and predictive modeling: Journal of Geophysical Research, 109, B02201, doi:10.1029/2003JB002566.

Patino, L.C., Carr, M.J., Feigenson, M.D., 2000, Local and regional variations in Central American arc lavas controlled by variations in subducted sediment input: Contributions to Mineralogy and Petrology, 138, 265-283.

Pawley, A.R., Holloway, J.R., 1993, Water source for subduction zone volcanism: new experimental constraints: Science, 260, 664-667.

Pearce, J.A., Peate, D.W., 1995, Tectonic implication of the composition of volcanic arc magmas: Annual Review of Earth and Planetary Sciences, 23, 251-285.

Peccerillo, A., Taylor, S.R., 1976, Geochemistry of Eocene calc-alkaline volcanic rocks from the Kastamonu area, Northern Turkey: Contributions to Mineralogy and Petrology, 58, 63-81.

Reiners, P.W., Hammond, P.E., McKenna, J.M., Duncan, R.A, 2000, Young basalts of the central Washington Cascades, flux melting of the mantle, and trace element signatures of primary arc magmas: Contributions to Mineralogy and Petrology, 138, 249-264.

Reynolds, R.W., Geist, D., 1995, Petrology of lavas from Sierra Negra volcano, Isabel Island, Galapagos Archipelago: Journal of Geophysical Research, B100, 24537-24553.

Sato, H., 1977, Nickel content of basaltic magmas and a measure of the degree of olivine fractionation: Lithos, 10, 113-120.

Saunders, A.D., Tarney, J., Weaver, S.D., 1980, Transverse geochemical variations across the Antarctic Peninsula: implications for the genesis of calc-alkaline magmas: Earth and Planetary Science Letters, 46, 344-360.

Schaaf, P., Heinrich, W., Besch, T., 1994, Composition and Sm-Nd isotopic data of the lower crust beneath San Luis Potosí, central Mexico: evidence from a granulite-facies xenolith suite: Chemical Geology 118, 63-84.

Schaaf, P., Stimac, J., Siebe, C., Macías, J.L., 2005, Geochemical evidence for mantle origin and crustal processes in volcanic rocks from Popocatépetl and surrounding monogenetic volcanoes, central Mexico: Journal of Petrology, 46, 1243- 1282.

Shapiro, L., Brannock, W.W., 1962, Rapid analyses of silicate, carbonate and phosphate rocks: Geological Survey Bulletin, 1144, 1–55.

Sheth, H.C., Torres-Alvarado, I.S., Verma, S.P., 2002, What is the "Calc-alkaline rock series"?: International Geology Review, 44, 686-701.

Shimoda, G., Tatsumi, Y., Nohda, S., Ishizaka, K., Jahne, B.M., 1998, Setouchi high-Mg andesites revisited: geochemical evidence for melting of subducting sediments: Earth and Planetary Science Letters, 160, 479–492.

Siebe, C., Rodríguez-Lara, V., Schaaf, P., Abrams, M., 2004a, Radiocarbon ages of Holocene Pelado, Guespalapa, and Chichinautzin scoria cones, south of Mexico City: implications for archaeology and future hazards: Bulletin of Volcanology, 66, 203–225.

Siebe, C., Rodríguez-Lara, V., Schaaf, P., Abrams, M., 2004b, Geochemistry, Sr-Nd isotope composition, and tectonic setting of Holocene Pelado, Guespalapa and Chichinautzin scoria cones, south of Mexico City: Journal of Volcanology and Geothermal Research, 130, 197-226.

Siebe, C., Arana-Salinas, L., Abrams, M, 2005, Geology and radiocarbon ages of Tláloc, Tlacotenco, Cuauhtzin, Hijo del Cuautzin, Teuhtli, and Ocusacayo monogenetic volcanoes in the central part of the Sierra Chichinautzin, México: Journal of Volcanology and Geothermal Research, 141, 225-243.

Siebert, L., Carrasco-Núñez, G., 2005, Late-Pleistocene to precolumbian behind-the-arc mafic volcanism in the eastern Mexican Volcanic Belt; implications for future hazards: Journal of Volcanology and Geothermal Research, 115 179-205.

Smith, D.R., Leeman, W.P., 2005, Chromian spinel–olivine phase chemistry and the origin of primitive basalts of the southern Washington Cascades: Journal of Volcanology and Geothermal Research, 140, 46-66.

Strong, M., Wolff, J., 2003, Compositional variations within scoria cones: Geology, 31, 143–146.

Sun, S.S., McDonough, W.F., 1989. Chemical and isotopic systematics of oceanic basalts: Implications for mantle composition and processes, *in* Saunders, A.D., Norry, M.J. (eds.), Magmatism in the Ocean Basins: Geological Society of London, Special Publication, 42, 313-345.

Swinamer, R.T., 1989, The geomorphology, petrography, geochemistry and petrogenesis of the volcanic rocks in the Sierra Chichinautzin, Mexico: Kingston, Queen's University, Master Thesis, 211 p.

Tatsumi, Y., 1989, Migration of fluids phases and genesis of basaltic magmas in subduction zones: Journal of Geophysical Research, 94(B4), 4697-4707.

Tatsumi, Y., 2001, Geochemical modeling of partial melting of subducting sediments and subsequent melt-mantle interaction: Generation of high-Mg andesites in the Setouchi volcanic belt, southwest Japan: Geology, 29(4), 323–326.

Tatsumi, Y., Sakuyama, M., Fukuyama, H, Kushiro I., 1983. Generation of arc basalt magmas and the thermal structure of the mantle wedge in subduction zones: Journal of Geophysical Research, 88(B7), 5815-5825.

Taylor, S.R., McLennan, S.M., 1985, The Continental Crust: its Composition and Evolution: Oxford, Blackwell, 321 p.

Tiepolo, M., Vannucci, R., Oberti, R., Foley, S., Bottazzi, P., Zanetti, A., 2000, Nb and Ta incorporation and fractionation in titanian pargasite and kaersutite: crystal-chemical constraints and implications for natural systems: Earth and Planetary Science Letters, 176, 185-201.

Tiepolo, M., Bottazzi, P., Foley, S., Oberti, R., Vannucci, R., Zanetti, A., 2001, Fractionation of Nb and Ta from Zr and Hf at mantle depths: the role of titanian pargasite and kaersutite: Journal of Petrology, 42, 221-232.

Toplis, M.J., 2005, The thermodynamics of iron and magnesium partitioning between olivine and liquid: criteria for assessing and predicting equilibrium in natural and experimental systems: Contributions to Mineralogy and Petrology, 149, 22-39.

Turner, S., Hawkesworth, C., Rogers, N., Bartlett, J., Worthington, T., Hergt, J., Pearce, J., Smith, I., 1997, ^{238}U-^{230}Th disequilibria, magma petrogenesis, and flux rates beneath the depleted Tonga-Kermadec island arc: Geochimica et Cosmochimica Acta, 61, 4855-4884.

Urrutia-Fucugauchi, J., Flores-Ruiz, J.H., 1996, Bouguer gravity anomalies and regional crustal structure in central Mexico: International Geology Reviews, 38, 176-194.

Vaggelli, G., Olmi, F., Conticelli, S., 1999, Quantitative electron microprobe analysis of reference silicate mineral and glass samples: Acta Vulcanologica, 11, 297–303.

van Bergen, M.J., Vroon, P.Z., Varekamp, J.C., Poorter, R.P.E., 1992, The origin of the potassic rock suite from Batu Tara Volcano (East Sunda Arc, Indonesia): Lithos 28, 261-282.

Velasco-Tapia, F., 2002, Aspectos geoestadísticos en geoquímica analítica: aplicación en el modelado geoquímico e isotópico de la Sierra de Chichinautzin, Cinturón Volcánico Mexicano: Universidad Nacional Autónoma de México, PhD Thesis, 273 p.

Velasco-Tapia, F., Verma, S.P., 2001a, First partial melting inversion model for a rift-related origin of Sierra de Chichinautzin volcanic field, central Mexican Volcanic Belt: International Geology Review, 43(9), 788-817.

Velasco-Tapia, F., Verma, S.P., 2001b, Estado actual de le investigación geoquímica en el campo monogenético de la Sierra de Chichinautzin: análisis de información y perspectivas: Revista Mexicana de Ciencias Geológicas 18, 168-203.

Verma, S.P., 1999, Geochemistry of evolved magmas and their relationship to subduction-unrelated mafic volcanism at the volcanic front of the central Mexican Volcanic Belt: Journal of Volcanology and Geothermal Research, 93, 151-171.

Verma, S.P., 2000, Geochemistry of subducting Cocos plate and the origin of subduction-unrelated mafic volcanism at volcanic front of central Mexican Volcanic Belt, *in* Delgado-Granados, H., Aguirre-Díaz, G.J., Stock, J. (eds.), Cenozoic tectonics and volcanism of Mexico: Boulder, Co. Geological Society of America, Special Paper, 334, 195-222.

Verma, S.P., 2002, Absence of Cocos plate subduction-related basic volcanism in southern Mexico: a unique case on Earth?: Geology, 30(12), 1095-1098.

Verma, S.P., Torres-Alvarado, I.S., Sotelo-Rodríguez, Z.T., 2002, SINCLAS: standard igneous norm and volcanic rock classification system: Computer and Geoscience, 28, 711-715.

Walker, J.A., Carr, M.J., Feigenson, M.D., Kalamarides, R.I., 1990, The petrogenetic significance of interstratified high- and low-Ti basalts in central Nicaragua: Journal of Petrology, 31, 1141-1164.

Walker, J.A., Patino, L.C., Carr, M.J., Feigenson, M.D., 2001, Slab control over HFSE depletions in central Nicaragua: Earth and Planetary Science Letters, 192, 533-543.

Wallace, P.J., Carmichael, I.S.E., 1999, Quaternary volcanism near the Valley of Mexico: implications for subduction zone magmatism and the effects of crustal thickness variations on primitive magma composition: Contributions to Mineralogy and Petrology, 135, 291-3140.

Wilson, M., 1989, Igneous Petrogenesis: A Global Tectonic Approach: Unwin Hyman, 466 p.

Workman, R.K., Hauri, E., Hart, S.R., Wang, J., Blusztajn, J., 2006, Volatile and trace elements in basaltic glasses from Samoa: Implication for water distribution in the mantle: Earth and Planetary Science Letters, 241, 932-951.

Xu, J.F, Ryuichi, S., Defant, M.J., Qiang, W.G., Rapp, R.P., 2002, Origin of Mesozoic adakitic intrusive rocks in the Ningzhen area of east China: Partial melting of delaminated lower continental crust?: Geology, 30, 1111-1114.

Zindler, A., Hart S. 1986, Chemical geodynamics: Annual Review of Earth and Planetary Sciences, 14, 493–571.

Manuscript received: May 16, 2007
Corrected manuscript received: January 10, 2008
Manuscript accepted: January 13, 2008